ACADÉMIE
DES SCIENCES
INSTITUT DE FRANCE

Comptes Rendus
Chimie

Clotilde Policar, Christine Rampon, Alice Balfourier, Michel Volovitch, Sophie Vriz, Hélène Charlotte Bertrand and Nicolas Delsuc

Inorganic chemical biology and metal complexes in cells: from the design of cellular models to evaluate antioxidant activity to the characterization of metal complexes in cells

Volume 28 (2025), p. 397-421

Online since: 16 April 2025

https://doi.org/10.5802/crchim.339

The Comptes Rendus. Chimie *are a member of the Mersenne Center for open scientific publishing*
www.centre-mersenne.org — e-ISSN : 1878-1543

ACADÉMIE DES SCIENCES
INSTITUT DE FRANCE

Comptes Rendus. Chimie
2025, Vol. 28, p. 397-421
https://doi.org/10.5802/crchim.339

Review article

Inorganic chemical biology and metal complexes in cells: from the design of cellular models to evaluate antioxidant activity to the characterization of metal complexes in cells

Clotilde Policar [*, a], Christine Rampon [a], Alice Balfourier [a], Michel Volovitch [a], Sophie Vriz [a], Hélène Charlotte Bertrand [a] and Nicolas Delsuc [a]

[a] Laboratoire Chimie physique et chimie du vivant, CPCV, UMR8228, Département de chimie de l'ENS-PSL, École normale supérieure, PSL University, Sorbonne Université, CNRS, 75005 Paris, France

E-mail: clotilde.policar@ens.psl.eu (C. Policar)

Abstract. Metal complexes are increasingly used as metallo-probes or metallo-drugs. Their characterization in cellular or biological environments poses specific challenges related to possible decoordination, metal exchange, fixation of additional ligands, or precipitation. These phenomena can hardly be foreseen and it is important to integrate the design of these complexes with their study in cells, from characterization in cells (quantification, speciation, integrity of the complex in cells, location) to bioactivity. Redox homeostasis and oxidative stress are strongly associated with biochemistry of metal ions. Metalloenzymes protecting against oxidative stress have evolved such as catalase or superoxide dismutase. Bioactive antioxidant metal complexes can be designed as catalysts bioinspired from these natural antioxidant enzymes protecting the cell against oxidative stress. To characterize their activity, it is important to develop dedicated cellular models to evaluate their ability to restore normal cell life from a situation compromised by oxidative stress. This article describes cellular models and assays that have been developed in that context as well as approaches to interrogate the complexes' nature in cells.

Keywords. Inorganic chemical biology, Oxidative distress, Integrity of complexes in cells, Speciation, Superoxide dismutase mimetics or mimics, Catalase mimics or mimetics.

Funding. ENS-PSL, PSL University, CNRS, MITI-CNRS, Sorbonne University (SU), ANR-15-CE07-0027 MAGIC; ANR-16-CE18-0017-01 SATIN; ANR-16-CE07-0025 Metallopepzyme; DEI20151234413 (Fondation pour la recherche médicale 2016), BACTMAN and ANACOMDA (Mission pour les initiatives transverses et interdisciplinaires MITI-CNRS), Association François Aupetit (AFA, research fellowship 2015), ANR 21-CE18-0053-02 MOBIDIC, ANR 20-CE07-0039-01-CATMAN, ANR 23-CE23 METALINFY; Idex PSL Qlife project Main ANR Q-life ANR-17-CONV-0005; CEFIPRA project no. 6505-1; EMERGENCE SU EMRG-24 TOTEM; ANR-22-PEBI-0003 (PEPR).

Note. Invited review on the occasion of the award to CP of the *Prix de la Fédération Gay-Lussac 2022* of the French *Académie des sciences*.

Manuscript received 17 May 2024, revised 9 July 2024, accepted 6 September 2024.

* Corresponding author

1. Introduction

Metal complexes have long been used as therapeutic agents. In the modern era, arsphenamine, toxic to syphilis-causing *Treponema pallidum*, or antimony compounds, toxic to leishmania, have been successfully developed as metal-based drugs in the early 20th century. However, most modern medicines are organic molecules. There has been a revival of inorganic medicinal chemistry with the discovery that *cis*-Pt can be toxic to cells with high division rate, with application as anticancer agent. Most of these compounds are meant to be used in living organisms and exert their activity at a cellular level. Because cells are compartmented, bioactivity can vary depending on the subcellular distribution and on the organelle reached. Cells are a very particular environment, with high viscosity, molecular overcrowding impacting diffusion [1], and abounding with metal cations and Lewis bases, which are strong competitors for metal cation coordination. This is why the use of metal complexes raises new specific challenges associated with possible decoordination, metal exchange, etc., that participate to their metabolization, with the possibility of precipitation when the metal cation is released. Predicting these exchanges is not easy due to the complexity of biological media. Exploring the integrity of a complex in cells is key to understanding its activity. Thus, it is important to integrate the design of metal complexes with their study in a cellular context, an approach for which the terms *cellular inorganic chemistry* or *inorganic chemical biology* can be coined [2].

Most of the metal complexes studied in the literature for their bioactivity are used as anticancer, antibacterial or antifungal agents, with requirements of selectivity—for cancerous cells, bacteria or fungi—versus normal healthy cells of the host. Hitherto, most bioanalyses have focused on evaluating the toxicity towards cancer cells, microorganisms, parasites, or fungi, which should be selective relative to vertebrate noncancerous cells. There is another class of metal complexes meant to restore the normal cellular life or rescue cells from a pathological or intoxication situation. This is the case for instance of functional mimics of rhodanese, an enzyme that detoxifies cyanide by catalyzing its conversion to thiocyanate [3,4]. Other catalytic metal-based drugs [5] can be developed to protect the cell from oxidative damages, as catalytic antioxidants mimicking protective enzymes such as superoxide dismutase (SOD) or catalase (CAT), called SOD mimics and CAT mimics [6–9]. Like the corresponding enzymes, these complexes are meant to catalytically react with reactive oxygen species (ROS), and do not act as inhibitors of ROS production. They must be nontoxic redox catalysts and they are meant to restore the basal activity in cells under oxidative distress. Their characterization therefore requires the development of specific non-routine strategies to evaluate their bioactivity, which is to restore normal cell life from a situation where it has been compromised [2,10–12]. Note also that, as activation of paramagnetic dioxygen (S = 1) can be performed by paramagnetic species, there is a strong intertwining between biochemistry of metal ions and metal complexes and that of dioxygen and ROS. This is why, in parallel with the development of SOD and CAT mimics, we have developed a particular interest in cellular models related to pathologies of oxidative stress that will be described in the following.

2. Oxidative stress, distress and eustress

Dioxygen (O_2) is necessary for aerobic life. Its ground state is S = 1 with two unpaired electrons in the highest occupied molecular orbital (HOMO). This diradical ground state nature (triplet state $^3O_2$) explains its slow reaction with organic molecules (mostly S = 0) [13]. O_2 sequential monoelectronic reductions lead to superoxide ($O_2^{\bullet -}$), hydrogen peroxide (H_2O_2) or hydroxyl radical ($HO^\bullet$), and then H_2O (see Figure 1). The partially reduced species—$O_2^{\bullet -}$, H_2O_2 and $HO^\bullet$—are much more reactive than dioxygen itself, with no spin-state kinetic barrier for the reaction with singlet molecules, and hence they are called *reactive oxygen species* (ROS). They are continuously produced in biological systems by endogenous mechanisms, and their concentration is maintained to low enough levels by protective pathways such as superoxide dismutase or catalase, proteins carved by evolution that catalyze respectively (7) and (8)[1].

[1]There has been so far no protective system identified for $HO^\bullet$: this radical reacts with a rate only limited by diffusion, meaning that the first encounter with a molecule leads to an efficient reac-

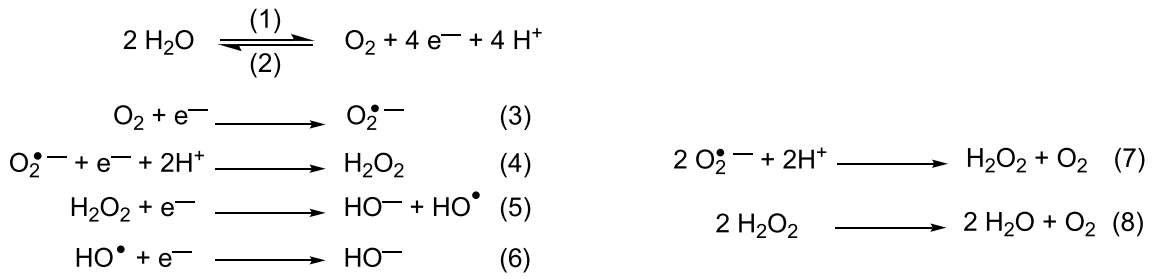

Figure 1. Oxidation of water (1) and reduction of dioxygen (2). Reduction cascade of O_2 leading to reactive oxygen species ROS (3) to (6). Dismutation of $O_2^{\bullet -}$ (7) and H_2O_2 (8). Note that the superoxide radical anion can be noted $O_2^{\bullet -}$ or O_2^-, the mention of the radical is not mandatory, as it is not in O_2 that could be noted $O_2^{\bullet\bullet}$ if we want to emphasize its diradical nature.

In the last two decades, it has become clear that cellular responses to redox imbalance are more complex than previously assumed. On the one hand, cells facing redox imbalance often react with an overshoot effect, as first evidenced in the case of reoxygenation after hypoxia [14]. On the other hand, it turned out that moderate oxidative imbalance (essentially due to spatially and temporally controlled H_2O_2 production) is used at different scales by cells and tissues as a signaling device to perform physiological tasks. Such signaling by H_2O_2 was, for instance, observed to be necessary for cytoskeleton rearrangement needed during migration [15,16], leukocyte navigation towards a wound [17], neural stem cell maintenance and neurogenesis [18,19], or tissue regeneration in fish or amphibian [20,21]. Among ROS, H_2O_2 is clearly suited to this signaling function due to its comparatively long half-life and thus diffusion properties, moderate reactivity, and membrane crossing ability via a subfamily of aquaporins. That is why H_2O_2 has been particularly studied as signaling molecule. To study its spatial distribution in real time, new genetically-encoded sensors have been developed (reviewed in [22], see also part 2.3 for the HyPer probe) [23,24]. These improved sensors allow analyzing the dynamics of redox balance in live organisms (reviewed in [25]). More recently they were used to revisit H_2O_2 dynamics and roles in neuronal differentiation [26], brain patterning [27], neuroinflammation [28], Shh signaling in the developing floor plate [29], appendage regeneration [30], and in hypoxia/reoxygenation [31]. Linking these findings with the observation that activation of several growth factors was accompanied by H_2O_2 production, H. Sies proposed the new concept of "oxidative eustress" [32–34]. According to this concept, H_2O_2 is a central redox signaling molecule in physiological contexts, transient and localized bursts of low levels of H_2O_2 (in the 1–10 nM range) being required for fundamental developmental and homeostatic processes from intracellular decisions to intercellular communication and organism patterning. In contrast, "oxidative distress" corresponding to supraphysiological levels of H_2O_2 (above 100 nM) definitely leads to various damages, with an intermediate range of concentration (from 10 to 100 nM) leading to adaptive stress responses.

3. A range of biological models to evaluate antioxidant activity

Metal complexes are of paramount importance for redox reactions, and they occupy a prominent position in the growing research field to fight oxidative stress. Metal complexes can be designed as antioxidants bioinspired by natural cellular antioxidants, such as SOD or CAT, leading to SOD mimics or CAT mimics able to catalyze the dismutation of $O_2^{\bullet -}$ and H_2O_2, respectively. Their chemical design has been discussed in the literature by us and others [6–9,35–38] and we will not focus on that aspect in the present article.

The evaluation of these mimics goes first through the characterization of their reactivity with either

tion (H-abstraction notably) and there is no possibility for this radical to diffuse to a protective system.

$O_2^{\bullet-}$ or H_2O_2 out of any cellular context, which we call *intrinsic activities*; this term refers therein to the reaction kinetics with $O_2^{\bullet-}$ or H_2O_2, possibly the catalytic constant in case of a true catalytic SOD/CAT mimic. But what will be mainly discussed in this section is the evaluation of the *bioactivities in cells*.

Many biological assays have been developed to characterize antioxidant activity of SOD and CAT mimics, ranging from fluorescent probes to SOD-deficient organisms [12,39,40]. We have been interested in the study of metal-based antioxidants in the context of inflammatory bowel diseases (IBDs). In that context, we have been developing three cellular models to evaluate the bioactivities of metal-based catalytic antioxidants, SOD or CAT mimics:

(a) activated macrophages [11,41].

(b) intestinal epithelial cells made highly sensitive to bacterial lipopolysaccharide (LPS, HT29-MD2 cells); the strong inflammation induced by LPS, presumably mediated by oxidative stress, is mitigated in the presence of SOD or CAT mimics [2,10,11,42].

(c) HyPer-HeLa cells genetically engineered to express a H_2O_2-sensing protein [11]; in these models we have characterized the bioactivity of a range of Mn-complexes described as SOD mimics in the literature [11].

3.1. *Evaluation of the effect of antioxidants on the superoxide ($O_2^{\bullet-}$) flow generated by macrophages*

Macrophages are immune cells meant to produce ROS against invading bacteria. High ROS flow can be induced upon stimulation with bacterial lipopolysaccharide (LPS), interferon γ (IFN-γ) and phorbol 12-myristate 13-acetate (PMA) (typically 24h, slow activation of the inducible NO synthase (iNOS) by LPS and IFN-γ followed by PMA, for the fast activation of the NADPH oxidase (NOX) (1h)) [41,43,44]. Quantification of $O_2^{\bullet-}$ concentration is made possible by using ferricytochrome *c* as a selective $O_2^{\bullet-}$ UV–vis marker. As cytochrome *c* is not able to penetrate cells, only the $O_2^{\bullet-}$ released extracellularly is measured [41,45]. Murine macrophages RAW 264.7 are first activated by LPS and IFN-γ for 24 hours. Cells are then incubated with PMA, ferricytochrome *c* and a chosen concentration of antioxidant that is nontoxic for the cells (typically estimated with a 3-(4,5-dimethylthiazol-2-yl)-2,5-diphenyl tetrazolium bromide (MTT) assay) in an homemade noncolored medium [11]. The absorbance of the supernatant at 550 nm, where there is a band for ferrocytochrome *c*, gives an estimate of the amount of $O_2^{\bullet-}$ in the extracellular medium (typically after 1h of incubation with ferricytochrome *c*) (see Figure 2). This assay was shown to provide a positive result with antioxidants not able to enter cells [11,41]. This is the case of the commercially available CuZnSOD, an efficient catalyst of the dismutation of $O_2^{\bullet-}$ into dioxygen and H_2O_2 with a kinetics close to diffusion limit. The CuZnSOD overall negative charge at physiological pH and its large size prevent its cell penetration when incubated in the extracellular medium. For that reason, we have labeled this experiment "extracellular activity assay" [11,41].

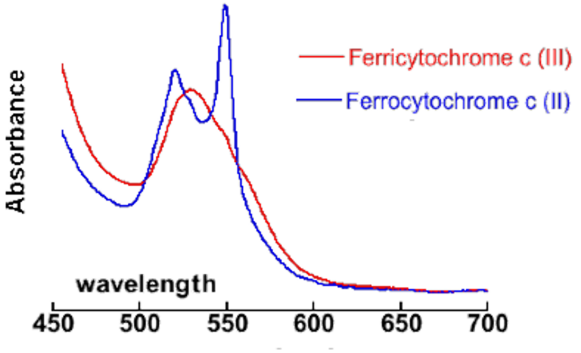

Figure 2. Visible spectrum (wavelength in nm) of ferri- and ferrocytochrome *c* showing the peak at 550 nm used for quantification.

The activity seen in this assay could be due either to (a) an inhibition of the $O_2^{\bullet-}$ production or (b) to the quenching of the superoxide produced (through a SOD-like activity). We have shown that the SOD mimic **Mn1** (see Figure 5) was not an inhibitor of $O_2^{\bullet-}$ production using an electrochemical quantification of ROS (H_2O_2, $ONOO^-$, NO, NO_2^-) with a possible back-calculation of the $O_2^{\bullet-}$ produced, which was similar with and without the **Mn1** incubation [41]. These results show that the reduction of the $O_2^{\bullet-}$ flow is not due to an inhibition of $O_2^{\bullet-}$ production, but to a direct reaction of **Mn1** with $O_2^{\bullet-}$. Note that the results in electrochemistry and by ferricytochrome *c* quantification were complementary, as the electrochemistry provides information on the overall $O_2^{\bullet-}$ production, not modi-

fied by the SOD mimic **Mn1**, and cytochrome *c* assay gives the extracellular flow of $O_2^{\bullet -}$ over a one-hour period, efficiently reduced by the presence of a SOD mimic [41].

3.2. *Epithelial intestinal cells as cellular models to estimate intracellular antioxidant and anti-inflammatory effects*

Oxidative stress is known to play a key role in triggering inflammation [46] and inflammatory bowel diseases [47]. Intestinal epithelial cells (IECs) have adapted to the presence of commensal bacteria with a limited response to bacterial lipopolysaccharide (LPS) of its regular receptor (TLR4). Low or absent expression of the myeloid differentiation 2 (MD2) receptor, LPS co-receptor to TLR4, underlies LPS tolerance in IECs, and MD2 blood circulating levels have been shown to be associated with LPS responsiveness [48,49]. The HT29 intestinal epithelial cell line has been stably transformed to overexpress the MD2 protein in the extracellular environment. The HT29-MD2 cell line thus exhibits a high LPS-responsiveness, increased more than 100-fold compared to the HT29 cell line [49,50]. The release of interleukin 8 (IL8), but also the expression of cyclooxygenase 2 (COX2) and the related secretion of prostaglandin E2 (PGE2), were coordinately stimulated by LPS in HT29 cells expressing MD2. We have also shown that LPS stimulation for six hours induces overexpression of an active mitochondrial MnSOD, but not of the cytosolic CuZnSOD nor CAT [2,10,11,51]. This is in line with LPS challenge–induced ROS production [52] at the mitochondria and clearly incriminates $O_2^{\bullet -}$. The overexpression of MnSOD has been interpreted as a result of cellular feedback to mitochondrial $O_2^{\bullet -}$ increase induced by LPS. In this cellular model, metal-based antioxidants displaying a SOD-like activity have shown anti-inflammatory activity, as measured by IL8 secretion and COX2 expression after six-hour incubation with LPS [2,10,11,51]. The expression of the MnSOD was reduced when LPS was co-incubated with a SOD mimic [2,10,11,42,51,53], showing that competent SOD mimics are able to complement for MnSOD.

A typical result with **Mn1** is shown in Figure 3. The anti-inflammatory activity of **Mn1** has been compared to the 5-aminosalicyclic acid (**5-ASA**, see Figure 5), an organic anti-inflammatory agent used as the first therapeutic line in IBD [2,54]. As shown on Figure 3, **5-ASA** is less efficient against inflammation than **Mn1**. A comparison of its antioxidant activity with other antioxidants, ranging from Mn porphyrins to organic nitroxide is discussed below (Table 1, Section 3.4 and Figure 7), showing that **Mn1** is among the best cell-efficient antioxidants.

3.3. *HeLa HyPer cells*

The detection of ROS using fluorescence probes is one of the most straightforward strategies to correlate the bioactivities of antioxidants with their intrinsic catalytic activities. However, for more reactive ROS such as the hydroxyl radical ($^{\bullet}OH$) and $O_2^{\bullet -}$, commercially available selective probes are scarce. Very interestingly, for H_2O_2 detection, a genetically encoded ratiometric sensor called HyPer has been developed, in HeLa cells among others [55]. HyPer is a circularly permuted yellow fluorescent protein (cpYFP) emitting at 530 nm, integrated into the regulatory domain of the bacterial H_2O_2-sensing protein OxyR (regulatory domain of OxyR, OxyR-RD). The oxidation of HyPer thiols by H_2O_2 induces the formation of disulfide bridges that leads to a modification of the spectral properties of the YFP. More precisely, a ratiometric modification of the excitation spectrum of HyPer, which possesses two excitation maxima at 420 and 488 nm, is induced. Thus, by measuring the normalized ratio of the intensity $I_{(405/530)}/I_{(491/530)}$ by confocal fluorescence microscopy, it is possible to monitor specifically H_2O_2 concentration in cells (see Figure 4). H_2O_2, being not as reactive as $O_2^{\bullet -}$, is able to diffuse across cytoplasmic membrane, mainly through aquaporines [56,57], and endogenous H_2O_2 diffuses outside cells. Consequently, when these HeLa HyPer cells are incubated with antioxidants mimicking CAT, the decrease in fluorescence ratio observed may be composite: it may be due to dismutation of endogenous H_2O_2 inside or outside the cells. For instance, incubation of HeLa HyPer with the recombinant heme CAT has been shown to reduce H_2O_2 concentration although it does not cross cells membrane [58]. When antioxidants possessing a CAT-like activity [11], including peptidyl Cu complexes (Figure 5) [24], were incubated with HeLa HyPer cells, a clear decrease in HyPer fluorescence has been observed, showing that they were efficient in this biological context [11,24].

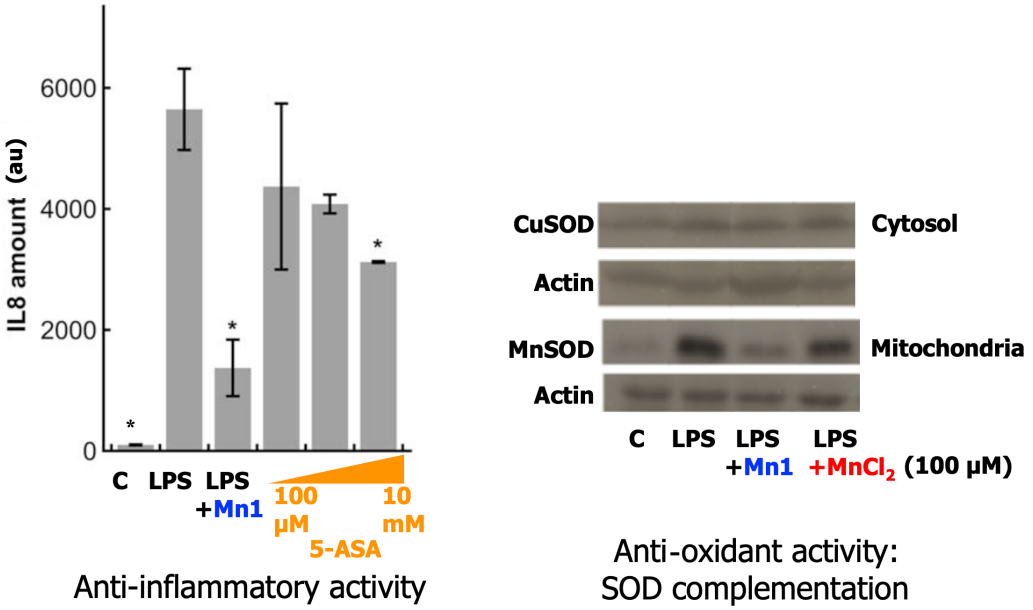

Figure 3. Anti-inflammatory and antioxidant activity of SOD mimic **Mn1** and comparison with 5-ASA (see Figure 5 for the structure of **Mn1** and 5-ASA). Left: Anti-inflammatory activity in intestinal epithelial cells activated with LPS: comparison with 5-ASA (see Figure 5). IL8 secretion measured by ELISA in supernatants of HT29-MD2 incubated 7 h under several conditions: C: control; LPS (0.1 µg/mL) was added after 1 h of incubation with **Mn1** (100 µM), **5 ASA**: 100 µM, 1 mM and 10 mM. Data represent means ± SD for 2 replicates, $^{**}p < 0.01$ and $^{*}p < 0.05$ versus LPS. Right: Antioxidant activity, measured indirectly by overexpression of MnSOD and CuSOD in comparison with actin. Representative experiment in Western blot (WB) after a 7 h incubation under several conditions, LPS (0.1 µg·mL^{-1}) added after 1 h and incubated for 6 h: C for control; LPS; LPS + **Mn1** (100 µM); LPS + $MnCl_2$ (100 µM). Adapted with permission from [2] Copyright 2017 American Chemical Society. These results are representative of typical experiments, performed many times by different experimentalists in slightly different conditions [2,10,11,51,53].

3.4. *Conclusion on the three cellular models*

We have recently used the above-mentioned extracellular assays to screen a range of antioxidants metal complexes known as SOD or CAT mimics (see Figure 5) [11].

We have compared their intrinsic activities, defined as their catalytic activities measured out of any cellular context, with their bioactivities in these assays (see Table 1).

Overall, three groups were identified for each of the assay, namely very efficient (++), efficient (+) and weakly active or inactive (−) antioxidants (Figure 6). As anticipated, the less intrinsically active antioxidants proved the most inactive in the cell assays. For instance, **MitoTempol** and **MnTBAP^{3-}**, which show a k_{cat} for superoxide activity lower than the rate of self-dismutation of superoxide and that are therefore not true SOD-like catalysts, were found inactive with the RAW model and HT29-MD2 assays. These two are probably able to react once with $O_2^{\bullet -}$ but their molecular structure or redox potential prevent cycling back and catalysis. In other words, they are stoichiometric antioxidants. The observation of their weak cellular activity is probably linked to their stoichiometric nature, as opposed to the higher activity catalytic antioxidants. In the extracellular assay (raw 264.7), the CuZnSOD was found to be very active as expected, but it was not active in the HT29-MDA assay: we can deduce that this assay (HT29-MD2) probes an intracellular antioxidant effect. For the HT29-MD2 assay, only **M40403**

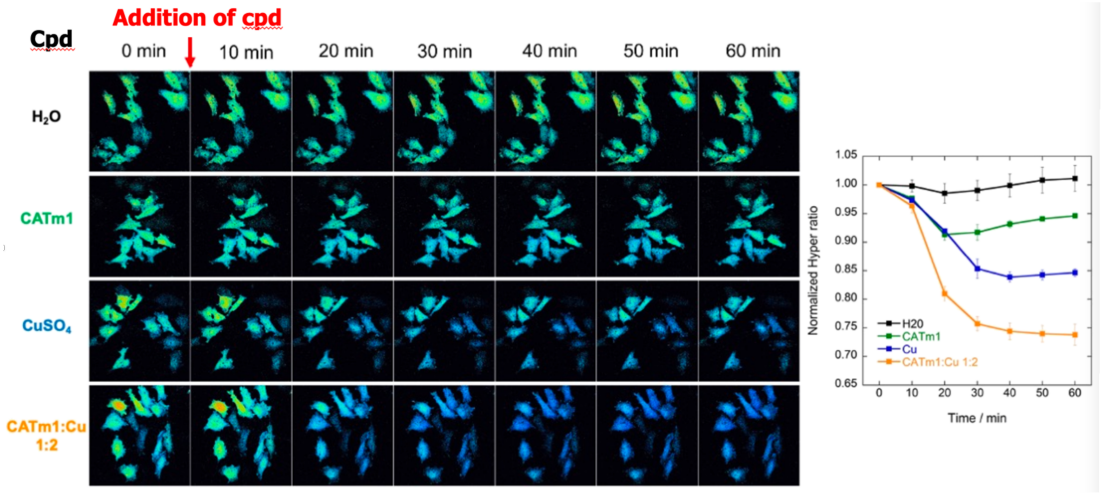

Figure 4. H_2O_2 levels in HeLa HyPer cells monitored by fluorescence for 60 min after treatment with H_2O (control cells), CATm1 peptide (250 μM), $CuSO_4$ (500 μM), and complex CATm1-Cu^{2+} 1:2 (250 μM). The right panel shows the mean ratio for 2 or 3 independent experiments. Adapted with permission from [24]. Copyright 2021 American Chemical Society.

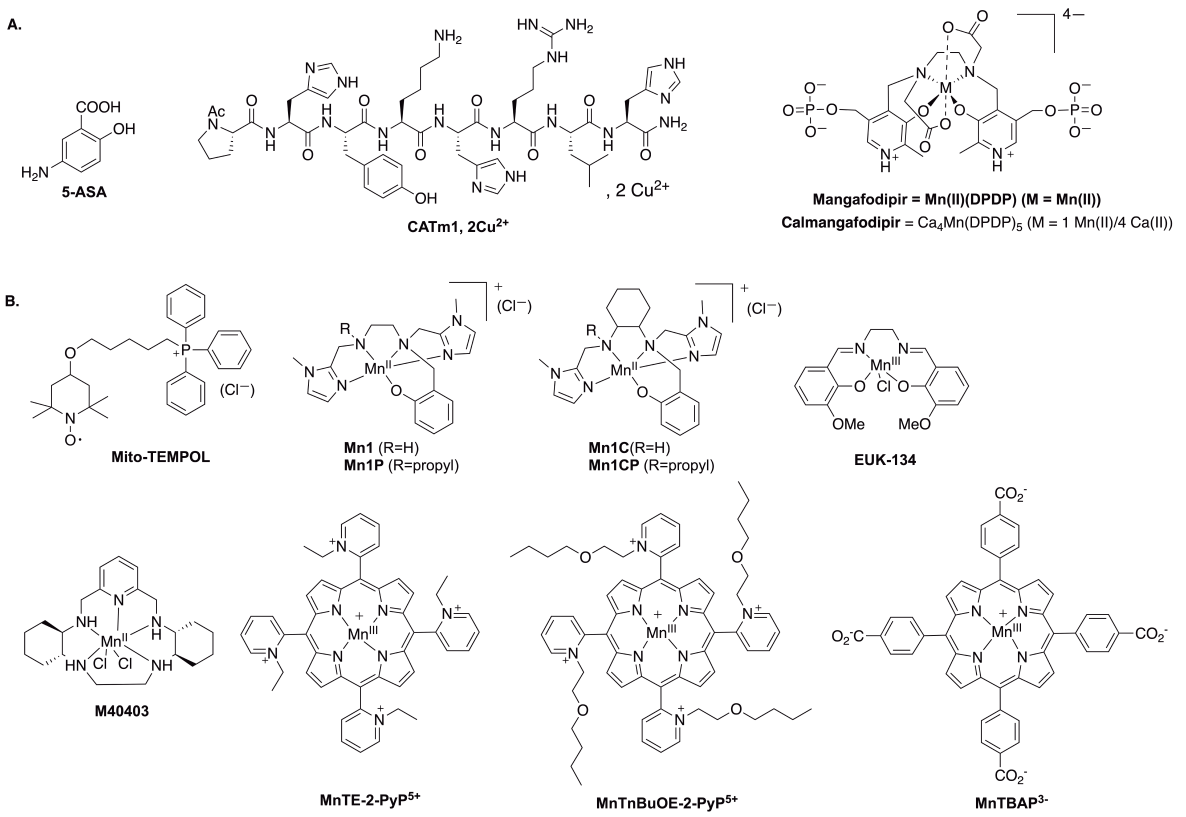

Figure 5. Chemical structures of the molecules discussed in this article. (A) **5-ASA**, **CATm1**, **Mangafodipir** and **Calmangafodipir**. (B) Structure of the antioxidants screened by the three-cell assay.

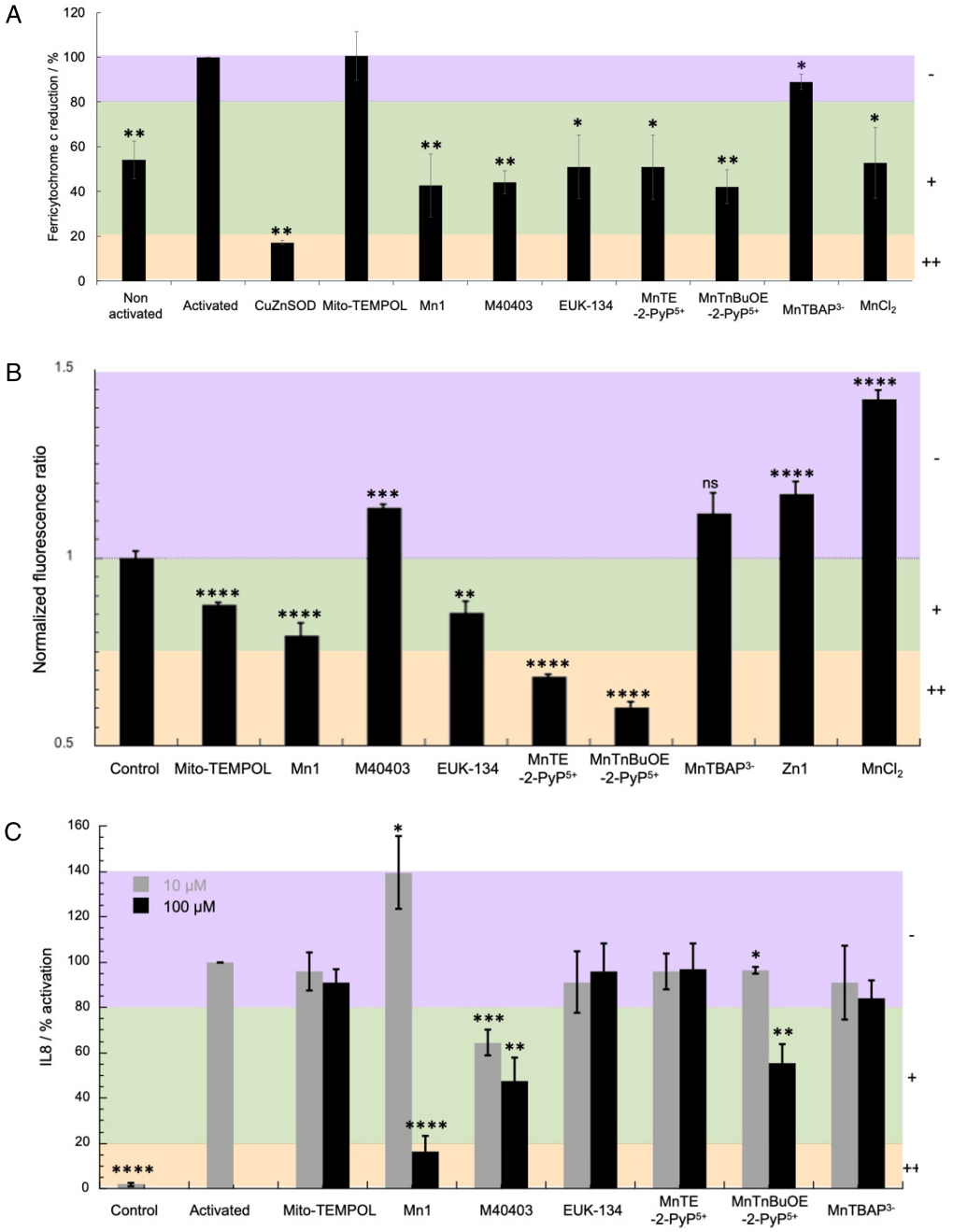

Figure 6. Screening of antioxidants with the three-cellular assay. Adapted with permission from [11]. Copyright 2021 Elsevier. (A) Evaluation of antioxidants on murine macrophages RAW 264.7. Relative values in comparison with activated cells arbitrarily set at 100%. Macrophages were incubated with IFN-γ (1 U·mL^{-1}) and LPS (1 ng·mL^{-1}) for 24 h at 37 °C in DMEM followed by an incubation with ferricytochrome *c* (100 µM), PMA (800 nM) and antioxidants (100 µM) at 37 °C for 1 h in a homemade medium devoid of phenol red (see [11] exp. Part). Data are mean ± SEM of three independent experiments with (**) $p < 0.01$ and (*) $p < 0.05$ versus activated cells. (B) H_2O_2 levels measured in HyPer HeLa cells.

Figure 6. (**cont.**) Cells were incubated for 1 h at 37 °C in HEPES (30 mM pH 7.5) under 5% CO_2 without (control) or with antioxidants at 100 μM. Fluorescence images were recorded after excitation at 405 nm and 491 nm and the ratio of the emission at 530 nm I(491/530)/I(405/530) was measured for several cells. The ratio was arbitrarily set to 1 for control cells, i.e., cells incubated with HEPES only. Data are mean ± SEM of several cells (from 48 to 163 cells) with $^{****}p < 0.0001$, $^{***}p < 0.001$, $^{**}p < 0.01$ and $^{*}p < 0.05$ versus control cells. ns means non-significant. (C) Quantification of the inflammatory marker IL8 by ELISA after incubation of HT29-MD2 cells with the antioxidants at 10 or 100 μM. Antioxidants were incubated for 6 h at 37 °C in supplemented DMEM in presence of LPS (0.1 $\mu g \cdot mL^{-1}$) except for control where neither antioxidants nor LPS were added. The absorbance measured for activated cells was arbitrary set to 100%. Data represent mean ± SEM of two independent experiments for **MnTnBuOE-2-PyP^{5+}** and **M40403** and three independent experiments for **Mito-TEMPOL**, **Mn1**, **EUK-134**, **MnTE-2-PyP^{5+}** and **MnTBAP^{3-}** with $^{****}p < 0.0001$, $^{***}p < 0.001$, $^{**}p < 0.01$ and $^{*}p < 0.05$ versus activated cells.

Table 1. Intrinsic dismutation kinetic constants and cellular activity of antioxidants

	SOD activity		CAT activity	Ref.	Macrophages	HT29-MD2		HeLa	Ref.
	k_{McCF} (10^6 $M^{-1}\cdot s^{-1}$)	k_{cat} (10^6 $M^{-1}\cdot s^{-1}$)	$k_{cat}H_2O_2$ ($M^{-1}\cdot s^{-1}$)[f]		(extracell)	10 μM	100 μM	HyPer	(cell assay)
Mito-TEMPOL	0.0297[a]		none		0	−	−	+	[11]
Mn1	7.0[b]	6.2[c] SF	2.3[g]	[59]	+	−	++	+	[11]
Mn1C	3.4[c]	nd	nd	[53]	nd	+	++	nd	[53]
M40403	3.55[b]	1.9[d] SF	8.2	[37,60,61]	+	+	+	−	[11]
EUK-134	0.602[b]	nd	13.0[h]	[37,62,63]	+	−	−	+	[11]
MnTE-2-PyP^{5+}	57[b]	54 PR	63.3	[37,64]	+	−	−	++	[11]
MnTnBuOE-2-PyP^{5+}	68[b]		88.5	[37,65]	+	−	+	++	[11]
MnTBAP^{3-}	0.00145[b]	none[d] SF	5.8	[61,65,66]	−	−	−	−	[11]
$MnCl_2$	1.3[b]	1.9[b] PR	none	[61,67,68]	+	nd	−	−	[11]
$Mn(ClO_4)_2$	1.3[b]			[69,70]	nd	nd	nd	nd	
CuZnSOD	692–1995[b]	2000[e] SF		[61,71–74]	++	(100 U/mL)	−	nd	
MnSOD		ca. 3000 PR		[75]	nd	nd	nd	nd	
Catalase			1.5×10^6	[37]	nd	nd	nd	nd	
Self-dismutation (pH 7.5)		0.3		[76,77]	nd	nd	nd	nd	

k_{McCF} refers to the rate constant calculated from the McCord and Fridovich assay [36,70].

[a]Ferricytochrome *c*, phosphate buffer (50 mM, pH 8). [b]Ferricytochrome *c*, phosphate buffer (50 mM, pH 7.8). [c]HEPES (60 mM, pH 7.4). [d] Phosphate buffer (50 mM, pH 7.4). [e]Phosphate buffer (50 mM, pH 7.8). [f]Unless specified, catalytic constants were measured by polarography using a Clark-type electrode in Tris buffer (50 mM, pH 7.8). [g]HEPES (100 mM, pH 7.4). [h]Value found for **EUK-8** instead of **EUK-134** which differs only by the two methoxy substituents. SF means stopped-flow and PR pulse radiolysis. [i]Cellular assays: + + / + / − refers to the level of activity in comparison with activated condition (macrophages and HT29-MD2) or basal H_2O_2 (HeLa HyPer) and they correspond to the color code in Figure 6. In blue: the best compounds identified as active in the three-cell assay.

and **MnTnBuOE-2-PyP^{5+}** were found active at both 10 μM and 100 μM, whereas **Mn1** was only active at 100 μM. Interestingly, more inert analogues of **Mn1**, **Mn1C** and **Mn1CP** were found to remain active at 10 μM [53], confirming the idea that the lack of activity of **Mn1** at 10 μM was due to its dissociation in cells (see below). A further study showed that, when **Mn1** dissociates in cells, it leads to the Zn-analogue, which was found inactive both in the HeLa HyPer and HT29-MD2 assays [42]. Another interesting example is the case of **MnTnBuOE-2-PyP^{5+}** and **MnTE-2-PyP^{5+}**, showing a similar intrinsic SOD activity and cell penetration but different bioactivities [11], probably due to different subcellular localizations.

Overall, the best compounds identified as active in the three-cell assay are those highlighted in blue in Table 1.

As we have already discussed in other cases [2,78,79], the overall efficacy of a metal-based compound relies on several parameters. Figure 7 shows radar plots revealing the link between intrinsic activity (bottom part) and cellular activities (upper part) determined in the three-cellular assays. The choice of axis was guided by the idea of maximizing the differences in the series explored, with favorable effects leading to a larger value on the axis (see caption of Figure 7 for details).

The cellular assays have been chosen for their complementarity, with the macrophage assay measuring the effect on the superoxide extracellular flow, HeLa Hyper measuring the effect on H_2O_2, and HT29-MD2 measuring an intracellular effect on inflammation induced by oxidative stress.

As shown on the upper-left insert in Figure 7, the upper part of the pentagons deciphers the biological effects on cells, whether extracellular (HeLa and macrophages, middle part of the pentagon) or intracellular (HT29-MD2 cell assay, at the apex of the pentagon), linked to oxidative stress in general.

The lower part reveals the intrinsic SOD and CAT activity. The left side of these pentagons is associated to the catalase-type activities (intrinsic and in the HeLa cell assay) and the right side with the anti-superoxide activities (intrinsic and in the macrophage assay).

The larger surface in the lower area, the higher the intrinsic activities. The larger the surface in the upper area, the better the activity in the three cells model. The larger the overall surface, the higher the antioxidants activities, intrinsic and in cells.

As shown by the analysis of Table 1 (see above), a low intrinsic activity leads to a weak cellular activity—see **Mito-TEMPOL** and **MnTBAP^{3-}** with the very small chart surface. For all compounds, the macrophage and HeLa cell assays, which probe a bioactivity in an extracellular medium, mirror well the intrinsic catalytic activities since cell penetration is not required. However, a large intrinsic activity (lower part of the pentagon) does not necessarily go with a high intracellular activity (HT29-MD2, apex of the pentagon). A loss of activity when going to cells or biological environment in general can be due to a low bioavailability, because of a weak penetration, poor stability in cells (see above, discussion in the case of **Mn1**), or formation of a less active ternary complex with cellular ligands.

MnTnBuOE-2-PyP^{5+} is the most active antioxidant followed by **MnTE-2-PyP^{5+}** and **Mn1** and this reflects on the surfaces of their pentagons being larger. The two porphyrins **MnTnBuOE-2-PyP^{5+}** and **MnTE-2-PyP^{5+}** are associated with a high intrinsic catalase and SOD activity. They show a similar good activity in the HeLa and macrophage assays but a weaker one in the HT29-MD2 assay. Note that the difference in activity between **MnTnBuOE-2-PyP^{5+}**, **MnTE-2-PyP^{5+}** and **MnTBAP^{3-}** cannot be ascribed to a difference in cell penetration. Indeed, **MnTBAP^{3-}**, anticipated to penetrate weakly due to its high negative charge, was paradoxically penetrating better in HT29-MD2 than **MnTnBuOE-2-PyP^{5+}** and **MnTE-2-PyP^{5+}** (see Figure 8). **Mn1** was the most penetrating molecule.

Mn1 has a very weak catalase activity and good SOD activity: this is shown by the surface on the chart representation being shifted to the right side. In contrast, the activity of **MnTnBuOE-2-PyP^{5+}**, **MnTE-2-PyP^{5+}** is more balanced between CAT and SOD, with a left-right symmetry of the filled inner surface.

These results on cells stress the importance of characterizing the bioactivity within cellular models. Of course, a compound needs to show a good intrinsic activity to be active in cells. But other parameters are at play, such as cell penetration, localization, stability, and inertia, in link with speciation in cells.

Other studies on Mn porphyrins have demonstrated that these compounds upregulate MnSOD, CAT, glutaredoxins (GRXs), peroxiredoxins (PRDXs) and other antioxidants. These proteins are under control of NRF2, a transcription factor known to activate genes through the antioxidant response element (ARE). NRF2 is continuously produced in cells and binds to KEAP1 (Kelch-like ECH-associated protein, ECH = enoyl-coenzyme A (CoA) hydratase) with a particular conformation that promotes its continuous degradation by the proteasome (see Figure 9). The modification of the Cys in KEAP1 (upon oxidative or chemical stress induced by electrophiles for instance) leads to an inhibition of NRF2 degradation: the newly synthesized NRF2 accumulates in the cytosol and translocates to the nucleus where it activates genes leading notably to an overexpression of SOD, CAT, glutathione reductase, heme-oxygenase

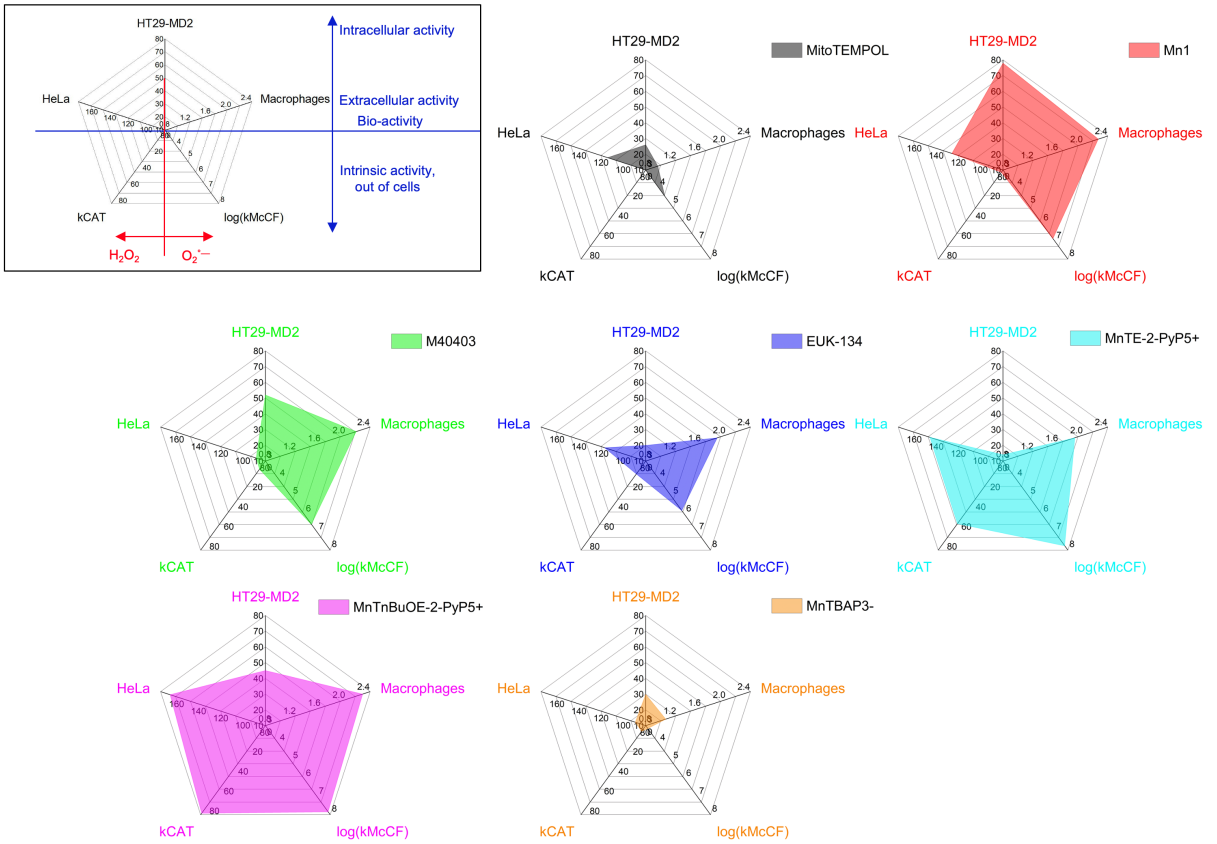

Figure 7. Performances of metal-based antioxidants compared using a radar representation for **MitoTEMPOL**, **Mn1**, **M40403**, **EUK-134**, **MnTBAP^{3-}**, **MnTnBuOE-2-PyP^{5+}**, and **MnTE-2-PyP^{5+}** after incubation at 100 µM. Upper-left radar: parameters involved in this representation. Axis c1: HeLa, 100/F (F = normalized fluorescence ratio, see Figure 6B). Axis c2: Macrophages, 100/F-red (F-red: % of ferricytochome *c* reduction, see Figure 6A). Axis c3: HT29-MD2, 100-I (I = IL8: % of activation by LPS, see Figure 6C).

(HO-1), and NAD(P)H dehydrogenase quinone (NQO1) [80]. Note that a similar activation of the ARE has also been proposed for nitroxides [81] which react stoichiometrically with $O_2^{\bullet-}$.

SOD mimics can then act through two pathways (see Figure 9) [9]: (A) by reducing the $O_2^{\bullet-}$ concentration and (B) by increasing H_2O_2 concentration leading to an induction of the ARE. The balance between these two pathways could depend on the speed of dismutation (k_{cat}, intrinsic activity) in comparison with the cellular capacity to detoxify H_2O_2 and also on the H_2O_2 cell content. A fast dismutation delivers a high shot of H_2O_2 concentration activating the antioxidant cellular response (pathway B, pro-oxidant). Pathway A may occur as soon as the SOD mimics enter the cells or the mitochondria but is also prone to decrease in time due to the SOD mimic degradation. In contrast, Pathway B requires time to activate protein synthesis (from 30 min to several hours), but this has a long-lasting effect as it works by boosting the cellular antioxidant feedback. We have recently shown by a proteomic cysteine-redoxomic analyses in HT29-MD2 that LPS challenge generates an early oxidative stress (15 min time-scale) leading to inflammation (hour time-scale) with a cellular-feedback activating the antioxidant response. These effects are mitigated by **Mn1** with an early limitation of the cysteine oxidations as early as 15 min [82].

In a way, compounds commonly known as SOD mimics can be separated into two classes [9]:

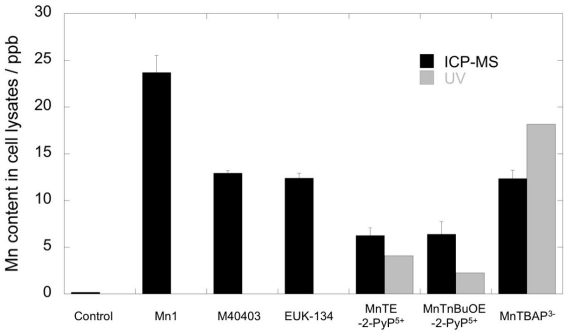

Figure 8. Quantification by inductively coupled plasma mass spectrometry (ICP-MS) (black columns) and UV spectrometry (gray columns, only for porphyrins) of Mn content in cell lysates of HT29-MD2 stimulated cells, incubated with or without compounds at 100 μM in DMEM supplemented with 10% heat-inactivated FBS and LPS (0.1 μg/mL). Values are given for a single experiment. For ICP-MS, values were corrected according to the Zn content of control cells to compare the data. Reprinted with permission from [11]. Copyright 2021 Elsevier.

(1) compounds directly acting on $O_2^{\bullet -}$, by catalyzing its dismutation, are truly mimicking SOD activity and should show an early cellular activity and (2) compounds, such as porphyrins, acting in fact as pro-oxidants, activate the cellular antioxidant enzymatic arsenal through transcription factors, such as NRF2, that promote gene expression of antioxidant proteins (SOD, CAT…). Their action takes longer to activate, as it depends on cellular protein biosynthesis, but also lasts longer.

3.5. *Of cells and mice*

3.5.1. *Mice models in link with inflammatory bowel diseases*

It has been shown that inflammation and oxidative stress are strongly intertwined in inflammatory bowels diseases (IBDs) [83]. In addition, IBDs are associated with a weakening of the antioxidant defenses: the content and/or activity of SODs was shown significantly reduced in plasma [84–86] or in tissues homogenates from resection specimen of IBD patients as compared to healthy subjects [87,88]. In this context, managing oxidative stress using SOD mimics is thus an interesting therapeutic alternative to existing treatments [89,90]. Toward this goal, we have used an IBD mouse model in which colitis is induced by administration of 2,4-dinitrobenzenesulfonic acid (DNBS). Starting the same day as DNBS administration, **Mn1** was administered daily by gavage in a basic buffer, to try to limit metal decoordination in the acidic stomach environment. Interestingly, mice treated with **Mn1** showed a significantly reduced weight loss in comparison with untreated mice, supporting the idea that accelerating superoxide dismutation is a valuable strategy against inflammatory pathologies [2]. Recently, we have shown that the anti-inflammatory activity of **Mn1** could be preserved in this mice colitis model, without using the buffer, when **Mn1** was loaded in bacteria (called “chemically modified bacteria”) [91].

3.5.2. *Side effects of anticancerous agents: mitigation of neuropathy by SOD mimics*

As already mentioned, low levels of ROS play important roles in normal cells and are involved in the regulation of cellular signaling and proliferation [92]. Higher levels of ROS along with deregulation of antioxidant pathways have been observed in cancer cells [92,93]. The differences in cellular redox states between normal and cancer cells and the role of ROS and their regulation in tumorigenesis have received much attention to explore and develop new therapeutic and preventive cancer-targeted strategies [94]. In the context of anticancer therapy, Mn-porphyrins SOD mimics have been studied in clinical trials for radioprotection of normal tissue and organ and for chemosensitization of cancer cells, their anticancer activity has been reviewed elsewhere [95,96].

Clinically used chemotherapeutics are characterized by dose-limiting off-target toxicities. Treatment with Oxaliplatin (Oxa), a reference drug in the treatment of digestive tract tumors, especially colorectal cancer and gastric cancer, is associated with the development of peripheral neuropathy (Oxa-induced peripheral neuropathy, OIPN) in a majority of patients in its acute form, which may evolve into a chronic form severely impacting the patients’ quality of life. OIPN is a frequent cause of treatment arrest and a major hurdle limiting Oxa’s clinical use with

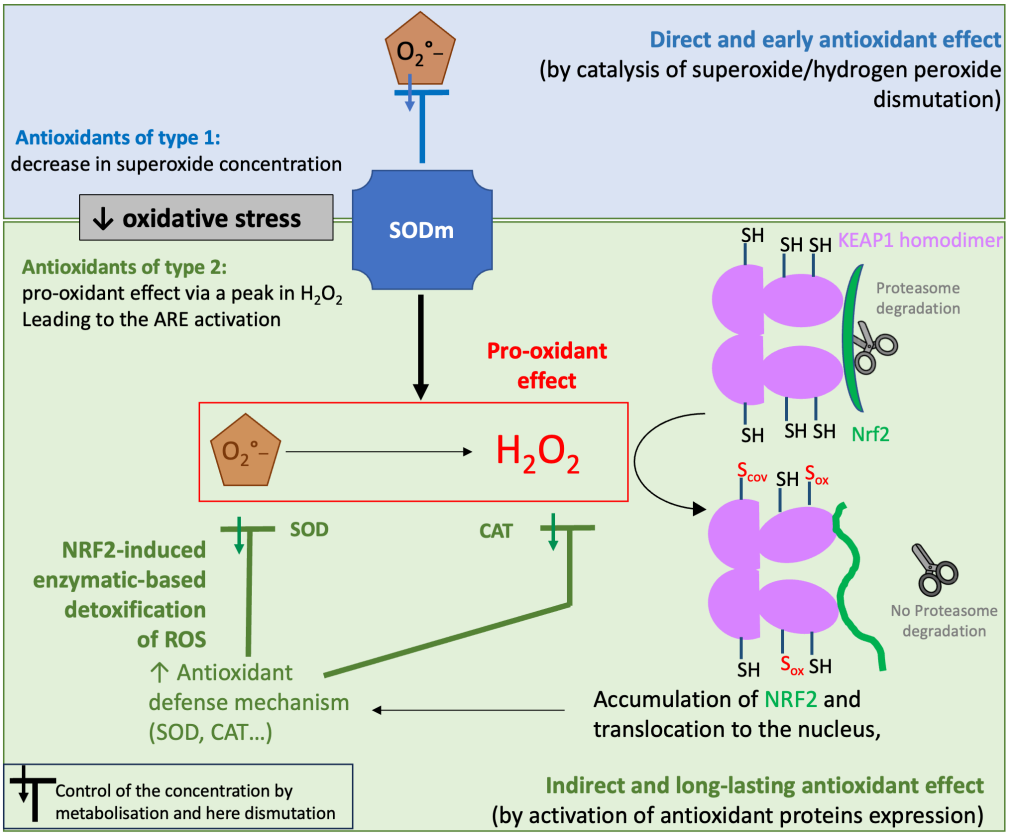

Figure 9. Schematic representation of the two possible pathways on cellular activity of SOD mimics. Pathway 1 corresponds to the direct effect of SOD mimics, with their ability to catalytically dismutate superoxide. A similar pathway could be ascribed to CAT mimics as well as they reduce H_2O_2. Pathway 2 is associated to a pro-oxidant effect of SOD mimics: as they produce H_2O_2, they can activate the NRF2-signaling ARE pathway involving the biosynthesis of antioxidant enzymes such as SOD. (Adapted with permission from [9].) Copyright 2022 Elsevier.

no clinically effective treatment or prevention therapy [97,98].

OIPN affects nerves and induces damages in peripheral nerves and dorsal root ganglia, causing pain, impaired sensations, or involuntary movements. The associated molecular mechanisms are complex and were shown to involve neuroinflammation, oxidative stress, and mitochondrial dysfunction. Antioxidants and modulators of redox balance have been studied as adjuvants in Oxa treatments in in vivo studies and were shown to have neuroprotective effects [99–101]. **Mangafodipir** (see Figure 5) is a Mn(II) complex developed for its activity as a contrast agent in magnetic resonance imaging (MRI), associated with the release of Mn(II) from the ligand, but which also shows SOD-like activity [102,103]. In this context, the first phase III neuroprotection trial in patients with colorectal cancer involved **calmangafodipir** (CaM; PledOx®; PledPharma AB/Egetis Therapeutics AB, see Figure 5), although negative results were reported [104].

We recently explored the relevance of SOD mimics derived from **Mn1** in combination treatments with Oxa in reducing OIPN [105,106]. In vitro, antitumoral activity was assessed by the viability and ROS production of tumor cell lines (CT16, HCT116, HT29) and murine fibroblasts (NIH3T3). In vivo, a murine model of colorectal cancer with subcutaneous injection of CT26 cells in Balb/c mice was used. The tumoral growth was monitored, and OIPN

was primarily assessed using a behavioral Von Frey test reflecting nociception and mechanical sensitivity (tactile pressure on the paw). In vivo, the association of **Mn1** derivatives to Oxa did not counteract Oxa's antitumoral activity, significantly decreased OIPN, and improved global clinical tolerance of Oxa. Additional effects were measured by cold plate tests, specific functional neuromuscular assays, and electron microscopy analyses of sciatic nerves. Further studies are on the way to characterize Pt accumulation in organs, peripheral nervous system, and tumors by inductively coupled plasma mass spectrometry (ICP-MS), and neuropathy markers by immunohistology (hind paws, sciatic nerves). Our studies showed that **Mn1** derivatives are promising in preventing the appearance of sensitive axonal neuropathy and neuromuscular disorders induced by Oxa [105,106], as they reduce Oxa-induced neurosensitive and neuromuscular alterations in vivo and prevent Oxa-induced peripheral demyelination. We are now developing covalent conjugates between Mn-SOD mimics and Oxa under the shape of Pt(IV) prodrugs and evaluating them for antitumoral activity and neuropathy prevention in mice models.

4. Speciation in cells: complex integrity and physical form

As exemplified by the results reported above, a key information when it comes to the design of bioactive metal complexes and rationalization of their bioactivity is their speciation. Speciation of an element is defined by the International Union of Pure and Applied Chemistry (IUPAC) as its distribution among defined chemical species, including molecular structure or physical form [107,108]. Determining the integrity of a metal complex within a biological system, or its physical form (solute, precipitate), is part of this description and several examples are given below.

Because it is not easy to anticipate which molecular structure is active in the biological environment, it is important to explore experimentally the nature of metal-based species present in cells. The recent development of analytical and imaging techniques [109,110], including X-ray fluorescence [9,111–113], nano secondary ion mass spectrometry (nanoSIMS) [109,110], ICP-MS and its laser ablation version for imaging (LA-ICP-MS) [109,114,115], ion mobility spectrometry coupled to mass spectrometry (IMS-MS) [42], Energy Dispersive X-ray (EDS or EDX) [116], or laser-induced breakdown spectroscopy (LIBS) [117], have bolstered our capacity of picturing the cellular content and distribution of metal based species and metal ions. We here delineate two original ways of examining the integrity of metal-complexes in cells, through X-fluorescence imaging and mass-based approaches. Molecular and chemical design tools have also been developed by chemists to improved stability and inertia of metal compounds [118–122]. In most cases, ligand exchange is being detrimental to the activity, but it can be also favorable and purposely designed, with a carrier metal complex delivering an active ligand, protected by metal coordination before reaching its target and then released in the desired cellular environment [123,124].

4.1. *Exploring complex integrity and speciation by "unconventional" methods*

4.1.1. *X-ray fluorescence imaging*

Exploring speciation in cells using a single imaging technique in a single experiment has the advantage of limiting sample manipulation (lysis, extraction, dilution, etc.), that could lead to metal decoordination, as much as possible. One original possibility is to use X-ray fluorescence (XRF), which enables the detection of heavy elements such as metal ions and imaging them using raster scanning of cells or biological tissue sections. If the ligand is appended with a heavy substituent, it is possible to map this heavy element as well as the metal ion and thus determine whether they colocalize in μ-XRF or not. This has been done for instance with a Br-substituted ligand [125].

We have functionalized a Mn-based SOD mimic with a rhenium-based moiety (see Figure 10). This type of Re-based complexes has been developed by us [126] and others, as UV–vis fluorescent probes. Interestingly, they also show IR and Raman characteristic absorptions and rhenium (Re) can be detected using X-fluorescence [113,127]. These probes are thus multimodal probes active in UV–vis fluorescence, IR, Raman, and X-fluorescence. The distribution of the Mn in cells incubated with **Mn1** is homogeneous in the cell (not shown) [2] and is different from that of **Mn1Re** with an accumulation into perinuclear organelles (see Figure 10) [10]. The Re-probe

is positively charged and hydrophobic: it may drive **Mn1Re** into lipid-rich organelles like mitochondria characterized by a negative potential [126]. The bioactivity in the HT29-MD2 assay (described above) of **Mn1** and **Mn1Re** was similar, although **Mn1Re** was overall more cell-penetrant than **Mn1**. Their anti-inflammatory activity is thought to be associated to a reduced LPS-induced mitochondrial oxidative stress. Interestingly, both **Mn1** and **Mn1Re** showed the same quantity accumulated in mitochondria, in line with their similar bioactivity and that bioactivity being associated with an effect in mitochondria.

4.1.2. *Metal speciation studied by mass spectrometry (MS) and ion mobility spectrometry (IMS)*

The detection and quantification of exogenous metal complexes are crucial to understand their activity in biological environments. In this regard, Mn(II) complexes are a challenge because of their low association constants, high lability, and rapid metal exchange [2,128,129]. We have recently shown that liquid chromatography coupled to mass spectrometry (LC-MS) in cell lysates can be used to detect and quantify Mn-based SOD mimics as long as they are not too labile, with the simple use of a calibration curve [53]. For the more labile ones, metal ions leaking from the LC-MS detection system were detrimental, with an Mn–Zn exchange, especially at low concentrations of the Mn complexes. As direct infusion showed no metal exchange, the leakage of metal ions from the separation part (LC) was incriminated to be responsible for the metal ion exchange (Mn–Zn) in the complex. Another separation technique, namely ion mobility, was then explored to separate labile metal complexes of the first transition series.

Ion mobility spectrometry (IMS) was first developed in the 1970s to detect traces of organic molecules in gas phase [130]. This technique uses separation according to the size of the molecule within an electric field and within a gas flow that pushes the molecules forward or backward depending on set-up. Their velocity is linked to their collision cross section (CCS). In IMS-MS, the detection is achieved by mass spectrometry. IMS-MS is a powerful technique used to characterize differences in folding of proteins upon ligand binding [131] or of peptides upon metal ion binding [132].

Recently, we have shown that IMS-MS is powerful enough to discriminate between very similar low molecular weight (LMW) ligands folding around metal ions across the first metal transition series [42]: ion mobility correlates well with ion radius (Figure 11). Then, IMS-MS was efficiently used to detect these labile metal complexes in cell lysates. They were quantified using a calibration curve with a standard made of a heavy ligand (with six ^{13}C) and a Co(II), metal ion chosen to lead to the least metal exchanges. The use of this heavy ligand-based Co complex, added just before IMS-MS analysis, allowed us to probe the metal exchange that occurred in the analytical system rather than in the cell lysates [42].

In the cellular context, there are a lot of Lewis bases that can coordinate to endogenous metal ions. The Irvin–Williams series [133] describes the range of association constants for divalent cations of the first transition row associated with unconstrained ligands. They show a trend of increasing association constant from left (Mn(II)) to right (Cu(II) and Zn(II)). Interestingly, Giedroc and Lisher have proposed a very enlightening idea, classifying cations as "competitive" (Zn(II), Cu(I), the redox state in cells) or "bioavailable" (Mn(II) but also, to a weaker extent, Fe(II)) [129]. Cu(I) and Zn(II) are more tightly controlled in cells than Mn(II). They show a higher association constant for most biological ligands. The existence of a pool of loosely bound Cu(I) and Zn(II) is very elusive, if only because hard to define. With a concentration of ca. 10^{-19} M estimated for this pool, as defined by the threshold of detection by endogenous metal sensors [134–136], this is not even one ion in a 2 pL cell, a typical volume for one eukaryotic cell. In contrast, the loosely bound pool is very abundant in Mn(II) (10^{-5} M corresponding to more than 10 millions Mn(II) ions in 2 pL) [129].

In a mixture where several metal ions M and several ligands L are competing, the primarily formed LM complex(es) are those showing the highest K_{LM} association constants. The ligands and metals ions remaining after this pairing are those less prone to associate. Hence, paradoxically, the stability threshold in cells is more stringent for Cu-complexes, which will find strong ligand competitors in cells, than for Mn-complexes, which will in contrast find Mn(II) highly bioavailable in cells. Furthermore, the loosely bound abundant pool of Mn(II) will contribute to shift the equilibrium M + L = LM toward the formation of the complex L–Mn(II). To that extent, and paradoxically, complexes of Mn(II), such as **Mn1**,

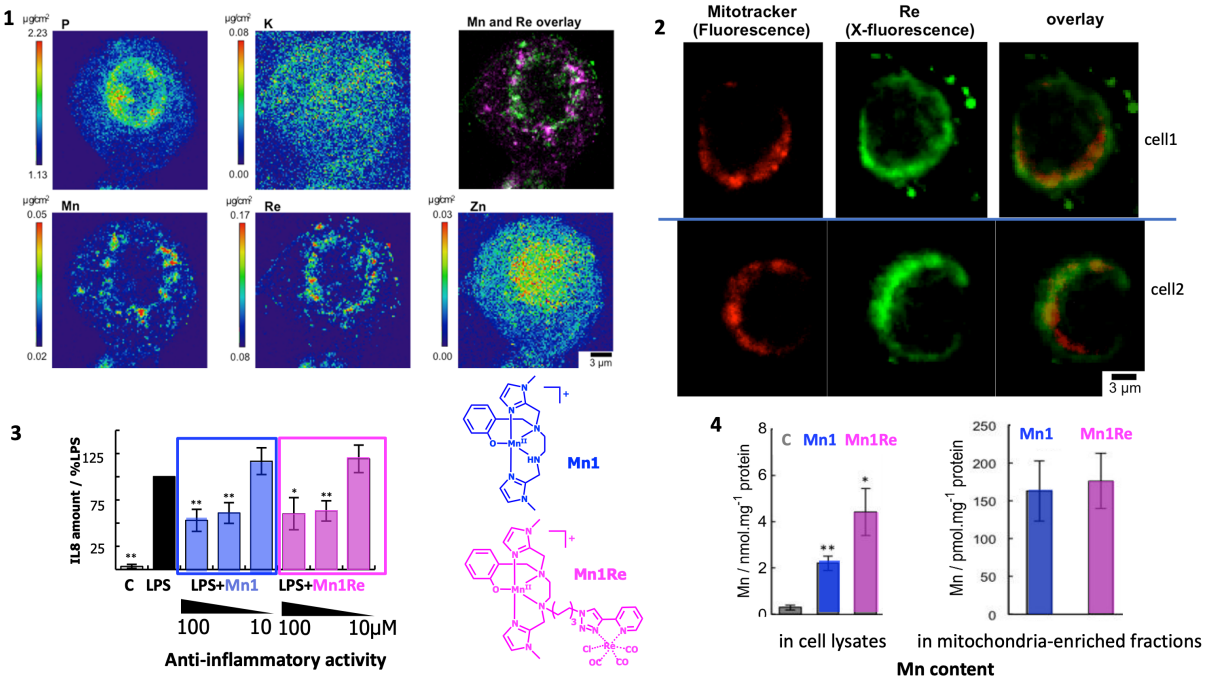

Figure 10. From ref [10]. (1) Elemental distribution of P, K, Mn, Re, and Zn in an HT29-MD2 cell incubated with **Mn1Re**. The phosphorus (P, Kα-line), and zinc (Zn, Kßz-line, and not Kα to avoid overlapping with Re Lα) maps are used to identify the nucleus area. The overlay (top right) corresponds to the manganese (Mn) (Kα-line) (magenta) and rhenium (Re) (Lß-line that does not overlap with other lines) (green) maps. The regions corresponding to an overlap of both elements are displayed in white. Intestinal epithelial cells HT29-MD2 were incubated for 2 h with **Mn1Re** (100 mM, 0.02% DMSO) before cryofixation and freeze-drying. Images were recorded on the 2-ID-D beamline of the APS synchrotron (excitation at 12.0 keV; integration time 2 s per pixel; pixel size 200 nm). (2) Confocal fluorescence images of HT29-MD2 of two different cells incubated with a mitochondrial marker (Mitotracker™, fluorescence) and X-fluorescence maps of **Mn1Re** (Re, X-fluorescence). Intestinal epithelial cells HT29-MD2 were incubated for 1.5 h with **Mn1Re** (100 µM, 0.02% DMSO) before the addition of Mitotracker™ deep red (200 nM, 30 min), washing with 50 mM EDTA, cryofixation and freeze-drying. Confocal fluorescence images of Mitotracker™ deep red (ex 633 nm, em 645–750 nm) were recorded with open pinhole. X-fluorescence (Re) images were recorded on the Nanoscopium beamline of SOLEIL synchrotron (excitation at 14.1 keV; integration time 2.4 s/pixel; pixel size 300 nm). Scale bar 3 µm. (3) C: control HT29-MD2 cells, **Mn1**/**Mn1Re**: HT29-MD2 cells incubated with **Mn1**/**Mn1Re** (10 and 100 µM, 6 h). IL8 secretion in HT29-MD2 cells. Intestinal epithelial cells HT29-MD2 were incubated for 7 h under different conditions indicated in the figure. LPS (0.1 $\mu g \cdot mL^{-1}$) was added at the end of the first hour. Data represent means +/− SEM for 7–10 independent experiments. (*) $p < 0.05$, (**) $p < 0.01$ vs. LPS condition. (4) C-control cells, **Mn1**/**Mn1Re**-HT29-MD2 cells incubated with **Mn1**/**Mn1Re** (100 µM, 6 h). Total Mn content was determined in acid-digested cell lysates by titration using EPR. Data represent mean +/− SEM for 4 independent experiments. (*) $p < 0.05$, (**) $p < 0.01$ versus C. Total Mn content in mitochondria-enriched fractions was determined by ICP-MS. Mitochondria were isolated using a mitochondria isolation kit (Thermo Fisher Scientific). Data represent mean +/− SEM for 7 independent experiments; see [11] for details. Schemes in blue and pink: molecular structure of **Mn1** and **Mn1Re** mentioned in this figure.

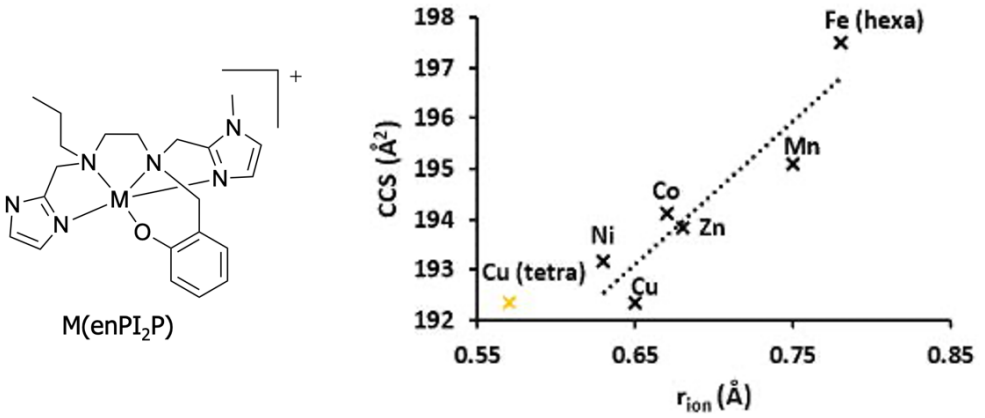

Figure 11. Collision cross-section of complexes **M(enPI$_2$P)** (M(II) coordinated by ligand enPI$_2$P) in Å^2 plotted against the ionic radius of metal cations in Å. The r_{ion} of any M(II) corresponds to a high-spin pentacoordination, except for Fe(II) (high-spin hexacoordination). The r_{ion} for Cu(II) is also shown (in yellow) for a high-spin tetracoordination. The r_{ion} values were taken from http://abulafia.mt.ic.ac.uk/shannon/ptable.php. Adapted with permission from [42]. Copyright 2022 Wiley.

Mn1P, **Mn1C** and **Mn1CP**, are probably ideal to be used in cells, as the ligand is weak enough not to compete with endogenous ligands for Cu or Zn (proteins), and probably strong enough to possibly remove Mn from the loosely bound endogenous Mn pool.

4.2. *Improving inertia against metal exchange*

As stated earlier, the use of metal complexes involving coordination bonds raises specific difficulties in terms of stability in biological contexts, associated with metal exchanges, ligand addition (into a ternary complex for instance) or ligand exchanges, which is in addition to questions raised by other metabolization pathways common with organic molecules. This can clearly impact the pharmacokinetics properties of metal complexes–based drugs. Indeed, the first metabolization pathway of such drugs is metal decoordination, in particular for complexes involving an open-chain ligand. Dissociation may occur via different pathways, such as spontaneous decoordination and acid-catalyzed or metal-assisted decomplexation involving exchange with a competitive metal ion [128]. Thermodynamic stability and kinetic inertness are thus key parameters to take into account when designing complexes for biological applications. In order to improve the biological properties of Mn(II)-based SOD mimics, inspired by the work of Tóth et al. [121], we have increased the inertness of the complexes by rigidifying the ligand central structure. To do so, the central ethane diamine bridge has been replaced by a trans cyclohexyl-1,2-diamine [53]. We expected that a weaker elasticity of the ligand, as defined by Comba [137], would reduce the kinetics of metal decoordination by limiting the opening–closing breathing. Indeed, we have shown that the rigidified ligand led to complexes with slower metal exchanges with divalent competitive cations [129] such as Cu^{2+}, Zn^{2+}, Ni^{2+}, and Co^{2+}. Very interestingly, this improved inertness was associated with similar to better anti-inflammatory and antioxidant properties in the HT29-MD2 cell line. These activities were also retained at lower concentration (10 μM, **Mn1C**, **Mn1CP**), than what is observed for the complex built with the unconstrained ligand (100 μM, **Mn1**). Increasing the inertness of complexes is consequently a valuable strategy to improve their bioactivities [53].

4.3. *Equilibrium between soluble and insoluble phases*

In addition to soluble species, it has also been observed that accumulated metals can form dense phases in biological systems, suggesting the formation of insoluble phases. This is particularly striking in the case of metal-accumulation diseases, such as hemochromatosis, i.e., iron (Fe) overload, or Wilson diseases, i.e., copper overload. In the

pathological contexts of metal overload, tissues that accumulate significant quantities of metals, such as the liver, generally present dense deposits of a few to few hundred nanometers. In the case of Fe, these phases can be identified as ferritin, the iron storage protein, resulting in the formation of crystalline objects around 8 nm, containing different crystalline phases [138]. However, not all metal ions undergo finely tuned biomineralization, and other transition metals could, when they accumulate, result in less organized phases, with differences in size, crystallinity, and composition. For example, in Wilson disease, while dense areas can easily be observed by transmission electron microscopy imaging, the diversity of the observed structures is important, and does not allow their nature to be clearly identified [139].

Interestingly, in a recent work published with Gazeau and Carn, we elucidated that exogenous metal ions could be subjected to precipitation as insoluble phases [140,141]. These observations stem from the initial description of the biodegradation of gold (Au) nanoparticles inside cell lysosomes. Not only was it found that Au nanoparticles evolve and dissolve over time, but that the released metal ions recrystallize under a unique ultrastructure, forming curved leaves composed of self-assembled nanometer-sized Au clusters. This was surprising as Au particles have been considered inert or non-degradable. However, this result was consistent with some old literature dedicated to soluble ionic Au compounds used for the therapy of rheumatoid arthritis [142]. In patients' biopsies and in animals, similar Au assemblies were observed due to Au accumulating in the tissues during treatment. These findings suggest that repeated exposure to an exogenous element in a soluble form can trigger its precipitation inside tissues as new solid phases with a common structure, regardless of the initial speciation of the metal (soluble, nanoparticular Au), the cell type considered, and the host species.

These phases present brand new challenges for speciation, as they present complex composition (mixed amorphous and crystalline phases incorporating endogenous elements, metabolites, or proteins) with complex reactivity, that can varies with the surrounding biological or chemical environment. They might also be highly sensitive to minor changes in their chemical environment, and particularly to change in the redox environment. Indeed, in the case of gold nanoparticles' biodegradation, oxidative stress was a key element to enable gold nanoparticles dissolution, and inhibition of intralysosomal ROS production was found to slow down degradation process [140]. Thus, lysosomal change in redox potential or pH might be of major importance in biodissolution processes, but also to the formation of insoluble phases.

If soluble–insoluble phase equilibrium raises new challenges to describe metals speciation, it also offers new opportunities for their characterization, as their density allows their observation using transmission or scanning electron microscopy, even if caution is called for as these highly energetic beams can destabilize the samples while observing [141,143].

This phenomenon of metal ions precipitation in biological matrices provides food for thought when considering how cells can deal with metal ions that are essential for their metabolism but become toxic at high concentration, such as iron and copper. Interestingly, it also raises questions about the metabolization of metal ions that are naturally present in ultra–trace levels, but become elevated due to exposure resulting from therapeutic, occupational, accidental or pollution-related activities. Indeed, precipitation could be a way for the cells to mitigate metal ion reactivity, limiting the proportion of chemically active atoms to the atoms accessible at the surface (which can be different from all of the surface atoms because of protein adsorption on the dense phase), thus also moderating their potential adverse effects.

5. Conclusion

Because speciation matters, integrating the design of metal complexes meant to be bioactive with their study in a cellular context is quite important and fruitful toward the development of therapeutic application for metal complexes. For this integrated approach, the terms cellular inorganic chemistry or inorganic chemobiology can be coined. It goes with a particular interest in subcellular metal imaging. In addition, as paramagnetic species such as metal centres perform activation of paramagnetic dioxygen, there is a strong intertwining between biochemistry of metal ions and that of dioxygen. In addition, metalloproteins and metal complexes are used to combat pathologies related to oxidative stress.

As it encompasses chemical conception, characterization, and cell studies, including chemical

analyses and evaluation of bioactivities, this approach in inorganic chemical biology requires skills in organic (ligands) and inorganic (complexes) syntheses, physical and analytical chemistries in intricate biological media, cell biology and bioimaging, with special interests in monitoring metal distribution and cell state, and more specifically redox state.

In this article we have described first the cellular models that we have developed for evaluating the bioactivities of these complexes. Those three cellular models can be used for the screening of metal-based antioxidants, to have a better idea of their propensity to act on superoxide or hydrogen peroxide concentration, and of their ability to be an efficient antioxidant in a biological context. The second part deals with the nature of the metal species in cells and of their subcellular distribution. The question of the integrity of metal complexes is intrinsically linked to the broader question of metal speciation, which aims to determine the complete array of metal-based species present, including insoluble phases formed by precipitation. Interestingly for the design of Mn-complexes, it is possible to play with the inertia to enhance bioactivity through a higher in-cell stability.

Abbreviations

ARE	Antioxidant response element
CaM	Calmangafodipir
CAT	Catalase
COX2	Cyclooxygenase 2
Cys	cysteine
DMEM	Dulbecco's modified eagle medium
DNBS	2,4-dinitrobenzenesulfonic acid
EDS/EDX	Energy-dispersive X-ray spectroscopy
EUK-134	See Figure 5
FBS	fetal bovine serum
GRX	glutaredoxin
HT29(-MD2)	Human colon cancer cell line (stably transfected to over express MD2, the co-receptor of TLR4 for LPS)
HeLa	Cancerous cell line
HEPES buffer	4-(2-hydroxyethyl)-1-piperazineethanesulfonic acid, pK_a (25 °C) = 7.48
HO	Heme oxygenase
HyPer	Hydrogen peroxide sensor
IBD	Inflammatory bowel diseases
ICP-MS/LA-ICP-MS	Inductively coupled plasma mass spectrometry/laser ablation inductively coupled plasma mass spectrometry
IEC	Intestinal epithelial cells
IFN-γ	Interferon γ
IL8	Interleukin 8
IUPAC	International union of pure and applied chemistry
IMS/MS	Ion mobility spectrometry coupled to mass spectrometry
KEAP1	Kelch-like ECH-associated protein
LC	Liquid chromatography
LIBS	Laser-induced breakdown spectroscopy
LPS	Lipopolysaccharide
LMW	Low molecular weight
MitoTempol	See Figure 5
MD2	Myeloid differentiation 2 (receptor)
Mn1, **Mn1C**, **Mn1CP**, **MnTxxx**, **M40403**	See Figure 5
MS	Mass spectrometry
MTT	3-(4,5-dimethylthiazol-2-yl)-2,5-diphenyl tetrazolium bromide
NAD(P)	Nicotinamide adenine dinucleotide (phosphate)
(i)NOS	(inductive) NO-synthase
NOX	NADPH oxidase
NQO-1	NAD(P)H Quinone Dehydrogenase 1
NRF2	Nuclear factor (erythroid-derived 2)-like 2
OIPN	Oxa-induced peripheral neuropathy
Oxa	OxaliPt
OxyR(-RD)	Bacterial peroxide sensor (regulatory domain)
PDRX	peroxiredoxin
PMA	Phorbol 12-myristate 13-acetate
PGE2	Prostaglandin E2
RAW 264.7	Murine macrophages
ROS	Reactive oxygen species
Shh	Sonic hedgehog
SIMS	Secondary ion mass spectrometry
SOD, CuZnSOD and MnSOD	Superoxide dismutase, Copper-Zinc superoxide dismutase, manganese superoxide dismutase; SOD1: SOD cytosolic (Cu-Zn); SOD2: MnSOD, mitochondrial

TLR4	Toll-Like-Receptor 4
Tris buffer	2-amino-2-(hydroxymethyl) propane-1,3-diol, pK_a (20 °C) = 8.3
XRF	X-fluorescence
(cp)YFP	(circularly permuted) yellow fluorescent protein

Declaration of interests

The authors do not work for, advise, own shares in, or receive funds from any organization that could benefit from this article, and have declared no affiliations other than their research organizations.

Funding

The authors want to acknowledge ENS-PSL, PSL University, CNRS, MITI-CNRS, Sorbonne University (SU) and the other bodies that funded this work. ANR-15-CE07-0027 MAGIC; ANR-16-CE18-0017-01 SATIN; ANR-16-CE07-0025 Metallopepzyme; DEI20151234413 (Fondation pour la recherche médicale 2016), and BACTMAN and ANACOMDA (Mission pour les initiatives transverses et interdisciplinaires MITI-CNRS), the Association François Aupetit (AFA, research fellowship 2015), ANR 21-CE18-0053-02 MOBIDIC, ANR 20-CE07-0039-01-CATMAN, ANR 23-CE23 METALINFY; Idex PSL Qlife project Main ANR Q-life ANR-17-CONV-0005; CEFIPRA project no. 6505-1; EMERGENCE SU EMRG-24 TOTEM; ANR-22-PEBI-0003 (PEPR).

Acknowledgements

Servier Medical Art, licensed under CC BY 4.0, is acknowledged for cell image used in TOC.

References

[1] D. Tsiapalis and D. I. Zeugolis, "It is time to crowd your cell culture media—physicochemical considerations with biological consequences", *Biomaterials* **275** (2021), article no. 120943.

[2] E. Mathieu, A.-S. Bernard, N. Delsuc, et al., "A cell-penetrant manganese superoxide dismutase (MnSOD) mimic is able to complement MnSOD and exerts an antiinflammatory effect on cellular and animal models of inflammatory bowel diseases", *Inorg. Chem.* **56** (2017), pp. 2545–2555.

[3] S. G. Suman, "Challenges in targeting cyanide poisoning: advantages in exploiting metal complexes in its treatment", in *Targeted Metallo-Drugs: Design, Development, and Modes of Action*, 1st edition (C. J. Marmion and E. Farkas, eds.), CRC Press: Boca Raton, 2023. Online at https://www.taylorfrancis.com/books/9781003272250 (accessed September 2, 2023).

[4] J. M. Gretarsdottir, I. H. Lambert, S. Sturup and S. G. Suman, "In vitro characterization of a threonine-ligated molybdenyl–sulfide cluster as a putative cyanide poisoning antidote; intracellular distribution, effects on organic osmolyte homeostasis, and induction of cell death", *ACS Pharmacol. Transl. Sci.* **5** (2022), pp. 907–918.

[5] J. J. Soldevila-Barreda and P. J. Sadler, "Approaches to the design of catalytic metallodrugs", *Curr. Opin. Chem. Biol.* **25** (2015), pp. 172–183.

[6] R. Bonetta, "Potential therapeutic applications of Mn-SODs and SOD-mimetics", *Chem. - Eur. J.* **24** (2018), pp. 5032–5041.

[7] S. Signorella, C. Palopoli and G. Ledesma, "Rationally designed mimics of antioxidant manganoenzymes: role of structural features in the quest for catalysts with catalase and superoxide dismutase activity", *Coord. Chem. Rev.* **365** (2018), pp. 75–102.

[8] I. Batinic-Haberle and I. Spasojevic, "25 years of development of Mn porphyrins—from mimics of superoxide dismutase enzymes to thiol signaling to clinical trials: the story of our life in the USA", *J. Porphyr. Phthalocyan.* **23** (2019), pp. 1326–1335.

[9] C. Policar, J. Bouvet, H. C. Bertrand and N. Delsuc, "SOD mimics: from the tool box of the chemists to cellular studies", *Curr. Opin. Chem. Biol.* **67** (2022), article no. 102109.

[10] E. Mathieu, A.-S. Bernard, E. Quévrain, et al., "Intracellular location matters: rationalization of the anti-inflammatory activity of a manganese (ii) superoxide dismutase mimic complex", *Chem. Commun.* **56** (2020), pp. 7885–7888.

[11] A. Vincent, M. Thauvin, E. Quévrain, et al., "Evaluation of the compounds commonly known as superoxide dismutase and catalase mimics in cellular models", *J. Inorg. Biochem.* **219** (2021), article no. 111431.

[12] G. Schanne, S. Demignot, C. Policar and N. Delsuc, "Cellular evaluation of superoxide dismutase mimics as catalytic drugs: challenges and opportunities", *Coord. Chem. Rev.* **514** (2024), article no. 215906.

[13] J. S. Valentine, J. Stubbe and M. Fontecave, "Dioxygen reactivity and toxicity", in *Biological Inorganic Chemistry* (I. Bertini, H. B. Gray, E. I. Stifel and J. S. Valentine, eds.), University Science Book: Sausalito, California, 2007, pp. 319–331.

[14] C. Li and R. M. Jackson, "Reactive species mechanisms of cellular hypoxia-reoxygenation injury", *Am. J. Physiol. Cell Physiol.* **282** (2002), pp. C227–C241.

[15] J.-S. Kim, T. Y. Huang and G. M. Bokoch, "Reactive oxygen species regulate a Slingshot–Cofilin activation pathway", *Mol. Biol. Cell* **20** (2009), pp. 2650–2660.

[16] D. Gianni, N. Taulet, C. DerMardirossian and G. M. Bokoch, "c-Src—mediated phosphorylation of NoxA1 and Tks4 induces the reactive oxygen species (ROS)—

dependent formation of functional invadopodia in human colon cancer cells", *Mol. Biol. Cell* **21** (2010), pp. 4287–4298.

[17] P. Niethammer, C. Grabher, A. Thomas Look and T. J. Mitchison, "A tissue-scale gradient of hydrogen peroxide mediates rapid wound detection in zebrafish", *Nature* **459** (2009), pp. 996–999.

[18] B. C. Dickinson, J. Peltier, D. Stone, D. V. Schaffer and C. J. Chang, "Nox2 redox signaling maintains essential cell populations in the brain", *Nat. Chem. Biol.* **7** (2011), pp. 106–112.

[19] J. E. Le Belle, N. M. Orozco, A. A. Paucar, J. P. Saxe, J. Mottahedeh, A. D. Pyle, H. Wu and H. I. Kornblum, "Proliferative neural stem cells have high endogenous ROS levels that regulate self-renewal and neurogenesis in a PI3K/Akt-dependant manner", *Cell Stem Cell* **8** (2011), pp. 59–71.

[20] C. Gauron, C. Rampon, M. Bouzaffour, E. Ipendey, J. Teillon, M. Volovitch and S. Vriz, "Sustained production of ROS triggers compensatory proliferation and is required for regeneration to proceed", *Sci. Rep.* **3** (2013), article no. 2084.

[21] N. R. Love, Y. Chen, S. Ishibashi, et al., "Amputation-induced reactive oxygen species are required for successful Xenopus tadpole tail regeneration", *Nat. Cell Biol.* **15** (2013), pp. 222–228.

[22] M. P. Murphy, H. Bayir, V. Belousov, et al., "Guidelines for measuring reactive oxygen species and oxidative damage in cells and in vivo", *Nat. Metab.* **4** (2022), pp. 651–662.

[23] C. Gauron, F. Meda, E. Dupont, et al., "Hydrogen peroxide (H_2O_2) controls axon pathfinding during zebrafish development", *Dev. Biol.* **414** (2016), pp. 133–141.

[24] K. Coulibaly, M. Thauvin, A. Melenbacher, et al., "A dicopper peptidyl complex mimics the activity of catalase, a key antioxidant metalloenzyme", *Inorg. Chem.* **60** (2021), pp. 9309–9319.

[25] C. Rampon, M. Volovitch, A. Joliot and S. Vriz, "Hydrogen peroxide and redox regulation of developments", *Antioxidants* **7** (2018), article no. 159.

[26] S. Albadri, F. Naso, M. Thauvin, et al., "Redox signaling via lipid peroxidation regulates retinal progenitor cell differentiation", *Dev. Cell* **50** (2019), 73–89.e6.

[27] I. Amblard, M. Thauvin, C. Rampon, et al., "H_2O_2 and engrailed 2 paracrine activity synergize to shape the zebrafish optic tectum", *Commun. Biol.* **3** (2020), article no. 536.

[28] J. Steudler, T. Ecott, D. C. Ivan, et al., "Autoimmune neuroinflammation triggers mitochondrial oxidation in oligodendrocytes", *Glia* **70** (2022), pp. 2045–2061.

[29] M. Thauvin, I. Amblard, C. Rampon, et al., "Reciprocal regulation of Shh trafficking and H_2O_2 levels via a non-canonical BOC-Rac1 pathway", *Antioxidants* **11** (2022), article no. 718.

[30] K. Chopra, M. Folkmanaitė, L. Stockdale, V. Shathish, S. Ishibashi, R. Bergin, J. Amich and E. Amaya, "Duox is the primary NADPH oxidase responsible for ROS production during adult caudal fin regeneration in zebrafish", *iScience* **26** (2023), article no. 106147.

[31] A. Zasu, F. Hishima, M. Thauvin, et al., "NADPH-oxidase derived hydrogen peroxide and Irs2b facilitate re-oxygenation-induced catch-up growth in zebrafish embryo", *Front. Endocrinol.* **13** (2022), article no. 929668.

[32] H. Sies, "Hydrogen peroxide as a central redox signaling molecule in physiological oxidative stress: oxidative eustress", *Redox Biol.* **11** (2017), pp. 613–619.

[33] H. Sies and D. P. Jones, "Reactive oxygen species (ROS) as pleiotropic physiological signalling agents", *Nat. Rev. Mol. Cell Biol.* **21** (2020), pp. 363–383.

[34] H. Sies, V. V. Belousov, N. S. Chandel, et al., "Defining roles of specific reactive oxygen species (ROS) in cell biology and physiology", *Nat. Rev. Mol. Cell Biol.* **23** (2022), pp. 499–515.

[35] O. Iranzo, "Manganese complexes displaying superoxide dismutase activity: a balance between different factors", *Bioorg. Chem.* **39** (2011), pp. 73–87.

[36] C. Policar, "Mimicking SODs, why and how: bio-inspired manganese complexes as SOD mimics", in *Redox Active Therapeutics* (I. Batinić-Haberle et al., ed.), Humana Press, Springer Nature: Switzerland, 2016, pp. 125–164.

[37] A. Tovmasyan, C. G. C. Maia, T. Weitner, et al., "A comprehensive evaluation of catalase-like activity of different classes of redox-active therapeutics", *Free Radic. Biol. Med.* **86** (2015), pp. 308–321.

[38] C. Policar, N. Delsuc and H. C. Bertrand, "Metal complexes in cells: from design of catalytic antioxidants to imaging metal ions and designing metal-based probes in X-ray fluorescence and IR-imaging, a multidisciplinary collaborative journey in bioinorganic chemistry and inorganic chemical biology", *C. R. Chim.* **27** (2024), pp. 1–25.

[39] A. Okado-Matsumoto, I. Batinić-Haberle and I. Fridovich, "Complementation of SOD-deficient Escherichia coli by manganese porphyrin mimics of superoxide dismutase activity", *Free Radic. Biol. Med.* **37** (2004), pp. 401–410.

[40] B. Kalyanaraman, M. Hardy and J. Zielonka, "A critical review of methodologies to detect reactive oxygen and nitrogen species stimulated by NADPH oxidase enzymes: implications in pesticide toxicity", *Curr. Pharmacol. Rep.* **2** (2016), pp. 193–201.

[41] A.-S. Bernard, C. Giroud, H. Y. Vincent Ching, et al., "Evaluation of the anti-oxidant properties of a SOD-mimic Mn-complex in activated macrophages", *Dalton Trans.* **41** (2012), pp. 6399–6403.

[42] M. Zoumpoulaki, G. Schanne, N. Delsuc, et al., "Deciphering the metal speciation in low-molecular-weight complexes by IMS-MS: application to the detection of manganese superoxide dismutase mimics in cell lysates", *Angew. Chem. Int. Ed.* **61** (2022), article no. e202203066.

[43] C. Amatore, S. Arbault, M. Guille and F. Lemaître, "Electrochemical monitoring of single cell secretion: vesicular exocytosis and oxidative stress", *Chem. Rev.* **108** (2008), pp. 2585–2621.

[44] M. R. Filipović, A. C. W. Koh, S. Arbault, et al., "Striking inflammation from both sides: Manganese(II) pentaazamacrocyclic SOD mimics act also as nitric oxide dismutases: a single-cell study", *Angew. Chem. Int. Ed.* **49** (2010), pp. 4228–4232.

[45] E. Njamkepo, F. Pinot, D. François, N. Guiso, B. S. Polla and M. Bachelet, "Adaptive responses of human monocytes infected by *Bordetella pertussis*: the role of adenylate cyclase hemolysin", *J. Cell. Physiol.* **183** (2000), pp. 91–99.

[46] B. Halliwell and J. M. C. Gutteridge, *Free Radicals in Biology and Medecine*, Oxford University Press: New York, 2007.

[47] E. Alemany-Cosme, E. Sáez-González, I. Moret, B. Mateos, M. Iborra, P. Nos, J. Sandoval and B. Beltrán, "Oxidative stress in the pathogenesis of Crohns disease and the interconnection with immunological response, microbiota, external environmental factors, and epigenetics", *Antioxidants* **10** (2021), article no. 64.

[48] J. Cosnes, C. Gower-Rousseau, P. Seksik and A. Cortot, "Epidemiology and natural history of inflammatory bowel diseases", *Gastroenterology* **140** (2011), pp. 1785–1794.

[49] C. Lenoir, C. Sapin, A. H. Broquet, et al., "MD-2 controls bacterial lipopolysaccharide hyporesponsiveness in human intestinal epithelial cells", *Life Sci.* **82** (2008), pp. 519–528.

[50] P. Seksik, H. Sokol, V. Grondin, et al., "Sera from patients with Crohn's disease break bacterial lipopolysaccharide tolerance of human intestinal epithelial cells via MD-2 activity", *Innate Immun.* **16** (2010), pp. 381–390.

[51] E. Mathieu, A.-S. Bernard, H. Y. Vincent Ching, et al., "Anti-inflammatory activity of superoxide dismutase mimics functionalized with cell-penetrating peptides", *Dalton Trans.* **49** (2020), pp. 2323–2330.

[52] G. Gloire, S. Legrand-Poels and J. Piette, "NF-κB activation by reactive oxygen species: fifteen years later", *Biochem. Pharmacol.* **72** (2006), pp. 1493–1505.

[53] G. Schanne, M. Zoumpoulaki, G. Gazzah, et al., "Inertness of superoxide dismutase mimics Mn(II) complexes based on an open-chain ligand, bioactivity, and detection in intestinal epithelial cells", *Oxid. Med. Cell. Longev.* **2022** (2022), article no. 3858122.

[54] A. Rezaie, R. D. Parker and M. Abdollahi, "Oxidative stress and pathogenesis of inflammatory bowel disease: an epiphenomenon or the cause?", *Dig. Dis. Sci.* **52** (2007), pp. 2015–2021.

[55] V. V. Belousov, A. F. Fradkov, K. A. Lukyanov, D. B. Staroverov, K. S. Shakhbazov, A. V. Terskikh and S. Lukyanov, "Genetically encoded fluorescent indicator for intracellular hydrogen peroxide", *Nat. Methods* **3** (2006), pp. 281–286.

[56] E. W. Miller, B. C. Dickinson and C. J. Chang, "Aquaporin-3 mediates hydrogen peroxide uptake to regulate downstream intracellular signaling", *Proc. Natl. Acad. Sci. USA* **107** (2010), pp. 15681–15686.

[57] G. P. Bienert, A. L. B. Møller, K. A. Kristiansen, A. Schulz, I. M. Møller, J. K. Schjoerring and T. P. Jahn, "Specific aquaporins facilitate the diffusion of hydrogen peroxide across membranes", *J. Biol. Chem.* **282** (2007), pp. 1183–1192.

[58] I. Amblard, M. Thauvin, C. Rampon, et al., "H_2O_2 and engrailed 2 paracrine activity synergize to shape the zebrafish optic tectum", *Commun. Biol.* **3** (2020), pp. 1–9.

[59] J. Trnka, F. H. Blaikie, A. Logan, R. A. J. Smith and M. P. Murphy, "Antioxidant properties of MitoTEMPOL and its hydroxylamine", *Free Radic. Res.* **43** (2009), pp. 4–12.

[60] I. Batinić-Haberle, J. S. Rebouças and I. Spasojević, "Superoxide dismutase mimics: chemistry, pharmacology, and therapeutic potential", *Antioxid. Redox Signal.* **13** (2010), pp. 877–918.

[61] F. C. Friedel, D. Lieb and I. Ivanović-Burmazović, "Comparative studies on manganese-based SOD mimetics, including the phosphate effect, by using global spectral analysis", *J. Inorg. Biochem.* **109** (2012), pp. 26–32.

[62] J. M. Pollard, J. S. Reboucas, A. Durazo, et al., "Radioprotective effects of manganese-containing superoxide dismutase mimics on ataxia–telangiectasia cells", *Free Radic. Biol. Med.* **47** (2009), pp. 250–260.

[63] S. Melov, S. R. Doctrow, J. A. Schneider, et al., "Lifespan extension and rescue of spongiform encephalopathy in superoxide dismutase 2 nullizygous mice treated with superoxide dismutase–catalase mimetics", *J. Neurosci.* **21** (2001), pp. 8348–8353.

[64] I. Batinić-Haberle, I. Spasojević, P. Hambright, L. Benov, A. L. Crumbliss and I. Fridovich, "Relationship among redox potentials, proton dissociation constants of pyrrolic nitrogens, and in vivo and in vitro superoxide dismutating activities of manganese(iii) and iron(iii) water-soluble porphyrins", *Inorg. Chem.* **38** (1999), pp. 4011–4022.

[65] I. Batinic-Haberle, A. Tovmasyan, E. R. H. Roberts, Z. Vujaskovic, K. W. Leong and I. Spasojevic, "SOD therapeutics: latest insights into their structure-activity relationships and impact on the cellular redox-based signaling pathways", *Antioxid. Redox Signal.* **20** (2014), pp. 2372–2415.

[66] J. S. Rebouças, I. Spasojević and I. Batinić-Haberle, "Pure manganese(III) 5,10,15,20-tetrakis(4-benzoic acid)porphyrin (MnTBAP) is not a superoxide dismutase mimic in aqueous systems: a case of structure–activity relationship as a watchdog mechanism in experimental therapeutics and biology", *J. Biol. Inorg. Chem.* **13** (2008), pp. 289–302.

[67] I. Spasojević, I. Batinić-Haberle, R. D. Stevens, P. Hambright, A. N. Thorpe, J. Grodkowski, P. Neta and I. Fridovich, "Manganese(III) biliverdin IX dimethyl ester: a powerful catalytic scavenger of superoxide employing the Mn(III)/Mn(IV) redox couple", *Inorg. Chem.* **40** (2001), pp. 726–739.

[68] K. Barnese, E. B. Gralla, D. E. Cabelli and J. Selverstone Valentine, "Manganous phosphate acts as a superoxide dismutase", *J. Am. Chem. Soc.* **130** (2008), pp. 4604–4606.

[69] C. Policar, S. Durot, F. Lambert, M. Cesario, F. Ramiandrasoa and I. Morgenstern-Badarau, "New MnII complexes with an N/O coordination sphere from tripodal N-centered ligands—characterization from solid state to solution and reaction with superoxide in non-aqueous and aqueous media", *Eur. J. Inorg. Chem.* **2001** (2001), pp. 1807–1818.

[70] S. Durot, C. Policar, F. Cisnetti, et al., "Series of Mn complexes based on N-centered ligands and superoxide - reactivity in an anhydrous medium and SOD-like activity in

an aqueous medium correlated to MnII/MnIII redox potentials", *Eur. J. Inorg. Chem.* **2005** (2005), pp. 3513–3523.

[71] S. Miriyala, I. Spasojevic, A. Tovmasyan, D. Salvemini, Z. Vujaskovic, D. St Clair and I. Batinic-Haberle, "Manganese superoxide dismutase, MnSOD and its mimics", *Biochim. Biophys. Acta - Mol. Cell Res.* **1822** (2012), pp. 794–814.

[72] S. Goldstein, I. Fridovich and G. Czapski, "Kinetic properties of Cu,Zn-superoxide dismutase as a function of metal content—Order restored", *Free Radic. Biol. Med.* **41** (2006), pp. 937–941.

[73] C. K. Vance and A. F. Miller, "A simple proposal that can explain the inactivity of metal-substituted superoxide dismutases", *J. Am. Chem. Soc.* **120** (1998), pp. 461–467.

[74] L. M. Ellerby, D. E. Cabelli, J. A. Graden and J. Selverstone Valentine, "Copper—Zinc superoxide dismutase: why not pH-dependent?", *J. Am. Chem. Soc.* **118** (1996), pp. 6556–6561.

[75] I. A. Abreu and D. E. Cabelli, "Superoxide dismutases—a review of the metal-associated mechanistic variations", *Biochim. Biophys. Acta - Proteins Proteom.* **1804** (2010), pp. 263–274.

[76] B. H. Bielski, D. E. Cabelli and R. L. Arudi, "Reactivity of $HO_2/O_2(-)$ radicals in aqueous solution", *J. Chem. Phys. Ref. Datat.* **14** (1985), pp. 1041–1100.

[77] D. Behar, G. Czapski, J. Rabani, L. M. Dorfman and H. A. Schwarz, "Acid dissociation constant and decay kinetics of the perhydroxyl radical", *J. Phys. Chem.* **74** (1970), pp. 3209–3213.

[78] Y. B. H. Hammouda, K. Coulibaly, A. Bathily, M. T. Sook Han, C. Policar and N. Delsuc, "Improvement of peptidyl copper complexes mimicking catalase: a subtle balance between thermodynamic stability and resistance towards H_2O_2 degradation", *Molecules* **27** (2022), article no. 5476.

[79] S. Clède, F. Lambert, R. Saint-Fort, M.-A. Plamont, H. Bertrand, A. Vessières and C. Policar, "Influence of the side-chain length on the cellular uptake and the cytotoxicity of rhenium triscarbonyl derivatives: a bimodal infrared and luminescence quantitative study", *Chem. - Eur. J.* **20** (2014), pp. 8714–8722.

[80] A. Tovmasyan, J. C. Bueno-Janice, M. C. Jaramillo, et al., "Radiation-mediated tumor growth inhibition is significantly enhanced with redox-active compounds that cycle with ascorbate", *Antioxid. Redox Signal.* **29** (2018), pp. 1196–1214.

[81] M. B. Y. Greenwald, S. Anzi, S. B. Sasson, H. Bianco-Peled and R. Kohen, "Can nitroxides evoke the Keap1–Nrf2–ARE pathway in skin?", *Free Radic. Biol. Med.* **77** (2014), pp. 258–269.

[82] M. Zoumpoulaki, G. Chiappetta, J. Bouvet, et al., "Kinetic redox shotgun proteomics reveals specific lipopolysaccharide effects on intestinal epithelial cells, mitigated by a Mn superoxide dismutase mimic", *Angew. Chem. Int. Ed.* (2025), article no. e202422644.

[83] S. Sedghi, J. Z. Fields, M. Klamut, et al., "Increased production of luminol enhanced chemiluminescence by the inflamed colonic mucosa in patients with ulcerative colitis", *Gut* **34** (1993), pp. 1191–1197.

[84] M. A. Alzoghaibi, I. A. Al-Mofleh and A. M. Al-Jebreen, "Antioxidant activities for superoxide dismutase in patients with Crohn's disease", *JBCPP* **25** (2014), pp. 59–62.

[85] M. Mrowicka, J. Mrowicki, M. Mik, Ł. Dziki, A. Dziki and I. Majsterek, "Assessment of DNA damage profile and oxidative/antioxidative biomarkers level in patients with inflammatory bowel disease", *Pol. J. Surg.* **92** (2020), pp. 1–5.

[86] K. Szczeklik, W. Krzysciak, R. Domagala-Rodacka, et al., "Alterations in glutathione peroxidase and superoxide dismutase activities in plasma and saliva in relation to disease activity in patients with Crohn's disease", *J. Physiol. Pharmacol.* **67** (2016), pp. 709–715.

[87] L. Kruidenier, I. Kuiper, W. van Duijn, S. L. Marklund, R. A. van Hogezand, C. B. H. W. Lamers and H. W. Verspaget, "Differential mucosal expression of three superoxide dismutase isoforms in inflammatory bowel disease", *J. Pathol.* **201** (2003), pp. 7–16.

[88] L. Kruidenier, I. Kuiper, W. Van Duijn, M. A. C. Mieremet-Ooms, R. A. van Hogezand, C. B. H. W. Lamers and H. W. Verspaget, "Imbalanced secondary mucosal antioxidant response in inflammatory bowel disease", *J. Pathol.* **201** (2003), pp. 17–27.

[89] F. Biasi, G. Leonarduzzi, P. I. Oteiza and G. Poli, "Inflammatory bowel disease: mechanisms, redox considerations, and therapeutic targets", *Antioxid. Redox Signal.* **19** (2013), pp. 1711–1747.

[90] S. M. Karp and T. R. Koch, "Oxidative stress and antioxidants in inflammatory bowel disease", *Disease-a-Month* **52** (2006), pp. 199–207.

[91] G. Schanne, A. Vincent, F. Chain, et al., "SOD mimics delivered to the gut using lactic acid bacteria mitigate the colitis symptoms in a mouse model of Inflammatory Bowel Diseases", *Free Radic. Res.* (2025). (accepted).

[92] V. Nogueira and N. Hay, "Molecular pathways: reactive oxygen species homeostasis in cancer cells and implications for cancer therapy", *Clin. Cancer Res.* **19** (2013), pp. 4309–4314.

[93] D. Trachootham, J. Alexandre and P. Huang, "Targeting cancer cells by ROS-mediated mechanisms: a radical therapeutic approach?", *Nat. Rev. Drug Discov.* **8** (2009), pp. 579–591.

[94] I. I. C. Chio and D. A. Tuveson, "ROS in cancer: the burning question", *Trends Mol. Med.* **23** (2017), pp. 411–429.

[95] I. Batinic-Haberle, A. Tovmasyan and I. Spasojevic, "Mn porphyrin-based redox-active drugs: differential effects as cancer therapeutics and protectors of normal tissue against oxidative injury", *Antioxid. Redox Signal.* **29** (2018), pp. 1691–1724.

[96] I. Batinic-Haberle, A. Tovmasyan, Z. Huang, et al., "H_2O_2-driven anticancer activity of Mn porphyrins and the underlying molecular pathways", *Oxid. Med. Cell. Longevity* **2021** (2021), pp. 1–23.

[97] T. Kawashiri, K. Mine, D. Kobayashi, M. Inoue, S. Ushio, M. Uchida, N. Egashira and T. Shimazoe, "Therapeutic agents for oxaliplatin-induced peripheral neuropathy; experimental and clinical evidence", *Int. J. Mol. Sci.* **22** (2021), article no. 1393.

[98] Y. Yang, B. Zhao, X. Gao, J. Sun, J. Ye, J. Li and P. Cao, "Targeting strategies for oxaliplatin-induced peripheral neuropathy: clinical syndrome, molecular basis, and drug development", *J. Exp. Clin. Cancer Res.* **40** (2021), article no. 331.

[99] R. Coriat, J. Alexandre, C. Nicco, et al., "Treatment of oxaliplatin-induced peripheral neuropathy by intravenous mangafodipir", *J. Clin. Invest.* **124** (2014), pp. 262–272.

[100] L. Di Cesare Mannelli, M. Zanardelli, I. Landini, et al., "Effect of the SOD mimetic MnL4 on in vitro and in vivo oxaliplatin toxicity: possible aid in chemotherapy induced neuropathy", *Free Radic. Biol. Med.* **93** (2016), pp. 67–76.

[101] A. Areti, V. G. Yerra, V. G. M. Naidu and A. Kumar, "Oxidative stress and nerve damage: role in chemotherapy induced peripheral neuropathy", *Redox Biol.* **2** (2014), pp. 289–295.

[102] J. O. G. Karlsson, L. J. Ignarro, I. Lundström, P. Jynge and T. Almén, "Calmangafodipir [Ca4Mn(DPDP)5], mangafodipir (MnDPDP) and MnPLED with special reference to their SOD mimetic and therapeutic properties", *Drug Discov. Today* **20** (2015), pp. 411–421.

[103] J. O. G. Karlsson, "Antioxidant activity of mangafodipir is not a new finding", *J. Hepatol.* **40** (2004), pp. 872–873.

[104] J. O. G. Karlsson, P. Jynge and L. J. Ignarro, "The damaging outcome of the POLAR phase III trials was due to avoidable time-dependent redox interaction between oxaliplatin and PledOx", *Antioxidants* **10** (2021), article no. 1937.

[105] C. Prieux-Klotz, H. Chédotal, M. Zoumpoulaki, et al., "A new manganese superoxide dismutase mimetic improves oxaliplatin-induced neuropathy and global tolerance in mice", *Int. J. Mol. Sci.* **23** (2022), article no. 12938.

[106] M.-A. Guillaumot, O. Cerles, H. C. Bertrand, et al., "Oxaliplatin-induced neuropathy: the preventive effect of a new super-oxide dismutase modulator", *Oncotarget* **10** (2019), pp. 6418–6431.

[107] D. M. Templeton, F. Ariese, R. Cornelis, L.-G. Danielsson, H. Muntau and H. P. Van Leeuwen, "IUPAC Recommendations 2000", *Pure Appl. Chem.* **72** (2000), pp. 1453–1470.

[108] T. Kiss, É. A. Enyedy, T. Jakusch and O. Dömötör, "Speciation of metal complexes of medicinal interest: relationship between solution equilibria and pharmaceutical properties", *Curr. Med. Chem.* **26** (2019), pp. 580–606.

[109] R. F. S. Lee, S. Theiner, A. Meibom, G. Koellensperger, B. K. Keppler and P. J. Dyson, "Application of imaging mass spectrometry approaches to facilitate metal-based anticancer drug research", *Metallomics* **9** (2017), pp. 365–381.

[110] J. Decelle, G. Veronesi, B. Gallet, et al., "Subcellular chemical imaging: new avenues in cell biology", *Trends Cell Biol.* **30** (2020), pp. 173–188.

[111] J. H. Lovett and H. H. Harris, "Application of X-ray absorption and X-ray fluorescence techniques to the study of metallodrug action", *Curr. Opin. Chem. Biol.* **61** (2021), pp. 135–142.

[112] J. Karges and N. Metzler-Nolte, "Advanced microscopy methods for elucidating the localization of metal complexes in cancer cells", in *Targeted Metallo-Drugs: Design, Development, and Modes of Action*, 1st edition (C. J. Marmion and E. Farkas, eds.), Metal Ions in Life Sciences Series, vol. 24 (A. Sigel, H. Sigel, R. Sigel, E. Freisinger, series eds.), CRC Press: Boca Raton, 2023, pp. 239–264.

[113] S. Hostachy, C. Policar and N. Delsuc, "Re(I) carbonyl complexes: multimodal platforms for inorganic chemical biology", *Coord. Chem. Rev.* **351** (2017), pp. 172–188.

[114] L. Mueller, A. J. Herrmann, S. Techritz, U. Panne and N. Jakubowski, "Quantitative characterization of single cells by use of immunocytochemistry combined with multiplex LA-ICP-MS", *Anal. Bioanal. Chem.* **409** (2017), pp. 3667–3676.

[115] J. Sabine Becker, "Imaging of metals in biological tissue by laser ablation inductively coupled plasma mass spectrometry (LA-ICP-MS): state of the art and future developments: imaging of metals by LA-ICP-MS", *J. Mass Spectrometry* **48** (2013), pp. 255–268.

[116] M. Scimeca, S. Bischetti, H. K. Lamsira, R. Bonfiglio and E. Bonanno, "Energy dispersive X-ray (EDX) microanalysis: a powerful tool in biomedical research and diagnosis", *Eur. J. Histochem.* **62** (2018), pp. 89–98.

[117] B. Busser, S. Moncayo, J.-L. Coll, L. Sancey and V. Motto-Ros, "Elemental imaging using laser-induced breakdown spectroscopy: a new and promising approach for biological and medical applications", *Coord. Chem. Rev.* **358** (2018), pp. 70–79.

[118] E. M. Gale, I. P. Atanasova, F. Blasi, I. Ay and P. Caravan, "A manganese alternative to gadolinium for MRI contrast", *J. Am. Chem. Soc.* **137** (2015), pp. 15548–15557.

[119] S. Laine, C. S. Bonnet, F. K. Kálmán, et al., "Mn^{2+} complexes of open-chain ligands with a pyridine backbone: less donor atoms lead to higher kinetic inertness", *New. J. Chem.* **42** (2018), pp. 8012–8020.

[120] D. Ndiaye, M. Sy, A. Pallier, et al., "Unprecedented kinetic inertness for a Mn^{2+}-bispidine chelate: a novel structural entry for Mn^{2+}-based imaging agents", *Angew. Chem. Int. Ed.* **59** (2020), pp. 11958–11963.

[121] D. Ndiaye, P. Cieslik, H. Wadepohl, A. Pallier, S. Même, P. Comba and É. Tóth, "Mn^{2+} bispidine complex combining exceptional stability, inertness, and MRI efficiency", *J. Am. Chem. Soc.* **144** (2022), pp. 22212–22220.

[122] M. Sy, D. Ndiaye, I. Da Silva, S. Lacerda, L. J. Charbonnière, É. Tóth and A. M. Nonat, "$^{55/52}Mn^{2+}$ complexes with a bispidine-phosphonate ligand: high kinetic inertness for imaging applications", *Inorg. Chem.* **61** (2022), pp. 13421–13432.

[123] T. W. Failes and T. W. Hambley, "Models of hypoxia activated prodrugs: Co(iii) complexes of hydroxamic acids", *Dalton Trans.* (2006), pp. 1895–1901.

[124] A. Glenister, C. K. J. Chen, D. J. Paterson, A. K. Renfrew, M. I. Simone and T. W. Hambley, "Warburg effect targeting Co(III) cytotoxin chaperone complexes", *J. Med. Chem.* **64** (2021), pp. 2678–2690.

[125] M. D. Hall, R. A. Alderden, M. Zhang, P. J. Beale, Z. Cai, B. Lai, A. P. J. Stampfl and T. W. Hambley, "The fate of platinum(II) and platinum(IV) anti-cancer agents in cancer cells and tumours", *J. Struct. Biol.* **155** (2006), pp. 38–44.

[126] R. A. J. Smith, C. M. Porteous, A. M. Gane and M. P. Murphy, "Delivery of bioactive molecules to mitochondria in vivo", *Proc. Natl. Acad. Sci. USA* **100** (2003), pp. 5407–5412.

[127] S. Clède and C. Policar, "Metal-carbonyl units for vibrational and luminescence imaging: towards multimodality", *Chem. Eur. J.* **21** (2015), pp. 942–958.

[128] B. Drahoš, J. Kotek, I. Cısařová, P. Hermann, L. Helm, I. Lukeš and É. Tóth, "Mn^{2+} complexes with 12-membered pyridine based macrocycles bearing carboxylate or phosphonate pendant arm: crystallographic, thermodynamic, kinetic, redox, and $^{1}H/^{17}O$ relaxation studies", *Inorg. Chem.* **50** (2011), pp. 12785–12801.

[129] J. P. Lisher and D. P. Giedroc, "Manganese acquisition and homeostasis at the host-pathogen interface", *Front. Cell. Infect. Microbiol.* **3** (2013), article no. 91.

[130] M. J. Cohen and F. W. Karasek, "Plasma chromatography—a new dimension for gas chromatography and mass spectrometry", *J. Chromatogr. Sci.* **8** (1970), pp. 330–337.

[131] E. Kalenius, M. Groessl and K. Rissanen, "Ion mobility–mass spectrometry of supramolecular complexes and assemblies", *Nat. Rev. Chem.* **3** (2019), pp. 4–14.

[132] Z. Du, R. E. F. de Paiva, K. Nelson and N. P. Farrell, "Diversity in gold finger structure elucidated by traveling-wave ion mobility mass spectrometry", *Angew. Chem. Int. Ed.* **56** (2017), pp. 4464–4467.

[133] H. Irving and P. Williams, "Order of stability of metal complexes", *Nature* **162** (1948), pp. 746–747.

[134] T. Nevitt, H. Öhrvik and D. J. Thiele, "Charting the travels of copper in eukaryotes from yeast to mammals", *Biochim. Biophys. Acta Mol. Cell Res.* **1823** (2012), pp. 1580–1593.

[135] A. Changela, K. Chen, Y. Xue, J. Holschen, C. E. Outten, T. V. O'Halloran and A. Mondragón, "Molecular basis of metal-ion selectivity and zeptomolar sensitivity by CueR", *Science* **301** (2003), pp. 1383–1387.

[136] N. J. Robinson and A. Glasfeld, "Metalation: natures challenge in bioinorganic chemistry", *J. Biol. Inorg. Chem.* **25** (2020), pp. 543–545.

[137] P. Comba, "Fit and misfit between ligands and metal ions", *Coord. Chem. Rev.* **238–239** (2003), pp. 21–29.

[138] M. C. Bessis and J. Breton-Gorius, "Iron Metabolism in the bone marrow as seen by electron microscopy: a critical review", *Blood* **19** (1962), pp. 635–663.

[139] L. Jonas, G. Fulda, T. Salameh, W. Schmidt, G. Kröning, U. T. Hopt and H. Nizze, "Electron microscopic detection of copper in the liver of two patients with Morbus Wilson by EELS and EDX", *Ultrastruct. Pathol.* **25** (2001), pp. 111–118.

[140] A. Balfourier, N. Luciani, G. Wang, et al., "Unexpected intracellular biodegradation and recrystallization of gold nanoparticles", *Proc. Natl. Acad. Sci. USA* **117** (2020), pp. 103–113.

[141] A. Balfourier, J. Kolosnjaj-Tabi, N. Luciani, F. Carn and F. Gazeau, "Gold-based therapy: from past to present", *Proc. Natl. Acad. Sci. USA* **117** (2020), pp. 22639–22648.

[142] F. N. Ghadially, *Ultrastructural Pathology of the Cell and Matrix*, Third edition, Elsevier: Amsterdam, 1988. Online at https://linkinghub.elsevier.com/retrieve/pii/C20130062470 (accessed February 21, 2024).

[143] A. Balfourier, E. Tsolaki, L. Heeb, et al., "Multiscale multimodal investigation of the intratissural biodistribution of iron nanotherapeutics with single cell resolution reveals co-localization with endogenous iron in splenic macrophages", *Small Methods* **7** (2023), article no. 2201061.